Unravelling the non-native low-spin state of the cytochrome c-cardiolipin complex: evidence of the formation of a His-ligated species only

Unravelling the non-native low-spin state of the cytochrome c – cardiolipin complex: evidence for the formation of a His ligated species only

Lisa Milazzo,[†] Lorenzo Tognaccini,[†] Barry D. Howes,[†] Federica Sinibaldi,[‡] Maria C. Piro,[‡] Maria Fittipaldi,[§] Maria C. Baratto,[≠] Rebecca Pogni,[≠] Roberto Santucci,[⊥] and Giulietta Smulevich[*,†]

[†]Dipartimento di Chimica "Ugo Schiff", Università di Firenze, Via della Lastruccia 3-13, 50019 Sesto Fiorentino, Italy

[‡]Dipartimento di Medicina Sperimentale e Chirurgia, Università di Roma 'Tor Vergata', Via Montpellier 1, 00133 Rome, Italy

[§]Dipartimento di Fisica ed Astronomia, Università di Firenze, Via Sansone 1, 50019 Sesto Fiorentino (FI), Italy

[≠]Dipartimento di Biotecnologie, Chimica e Farmacia, Università di Siena, via Aldo Moro 2, 53100 Siena, Italy

[⊥]Dipartimento di Scienze Cliniche e Medicina Traslazionale, Università di Roma 'Tor Vergata', Via Montpellier 1, 00133 Rome, Italy

Corresponding Author

*Phone: +39-055-4573083. E-mail: giulietta.smulevich@unifi.it.

Running title: Bis-His formation in the cytochrome c-cardiolipin complex

Keywords: apoptosis; misligation; resonance Raman; EPR; site directed mutagenesis.

Funding

This work was supported by MIUR PRIN 2010C4R8M8 (G.S.) and Ente Cassa Risparmio di Firenze, Grant No. 2014-0100 (G.S.).

Abbreviations

5c, penta-coordinated heme state; 6c, hexa-coordinated heme state; CL, cardiolipin; Cyt c, cytochrome c; E, elephant; EPR, electron paramagnetic resonance; H2633N, horse heart Cyt c His26Asn/His33Asn double mutant; HPLC, high-performance liquid chromatography; HS, high-spin; K727379N, horse heart Cyt c Lys72Asn/Lys73Asn/Lys79Asn triple mutant; K7273N/H26Y, horse heart Cyt c Lys72Asn/Lys73Asn/His26Tyr triple mutant; K7273N/H33Y, horse heart Cyt c Lys72Asn/Lys73Asn/His33Tyr triple mutant; LS, low-spin; Mb, myoglobin; RR, resonance Raman; SDS, sodium dodecyl sulfate; SDS-PAGE, sodium dodecyl sulphate - polyacrylamide gel electrophoresis; SW, sperm whale; SW H64V, sperm whale myoglobin His64Val mutant; WT, wild type.

Notes

The authors declare no competing financial interest

Author Contributions

All authors conceived and designed the experiments. LM, LT, BDH, FS, MCP, MF, MCB, RP, RS performed the experiments. All authors analyzed the data, and contributed reagents/materials/analysis tools. BDH and GS wrote the paper.

ABSTRACT

The interaction between cytochrome c (Cyt c) and cardiolipin (CL) plays a vital role in the early stages of apoptosis. The binding of CL to Cyt c induces a considerable increase in its peroxidase activity that has been attributed to the partial unfolding of the protein, dissociation of the Met80 axial ligand and formation of non-native conformers. Although the interaction between Cyt c and CL has been extensively studied, there is still no consensus regarding the conformational rearrangements of Cyt c that follow the protein-lipid interaction. To rationalize the different results and gain better insight into the Cyt c-CL interaction, we have studied the formation of the CL complex of the horse heart wild type protein and selected mutants in which residues considered to play a key role in the interaction with CL (His26, His33, Lys72, Lys73, Lys79) have been mutated. The analysis was conducted at both room and low temperature via UV-vis absorption, resonance Raman, and electron paramagnetic resonance spectroscopies. The trigger and the sequence of CL-induced structural variations is discussed in terms of disruption of the His26−Pro44 hydrogen bond. We unequivocally identify the sixth ligand in the partially unfolded, non-native low spin state that Cyt c can adopt following the protein-lipid interaction, as a His ligation, ruling out the previously proposed involvement of a Lys residue or an OH^- ion.

Cytochrome c (Cyt c) is a multiple function mitochondrial protein that plays an important role both in electron transfer and in programmed cell death (apoptosis). It is well-known that cardiolipin (CL), a phospholipid of the inner mitochondrial membrane, mediates the anchoring of Cyt c to the inner mitochondrial membrane for electron transfer during respiration and also participates in the steps preceding apoptosis.[1,2] To perform the former task, the protein must adopt its native fully folded state in which the axial sulphur atom of Met80 serves as the sixth distal ligand of the heme iron. It has been recently proposed that relaxation of the native Cyt c heme ruffling distortion to a more planar state when bound to the mitochondrial membrane may act as a "switch", making it easier for the protein to accept electrons when membrane bound than when it is free in the cytoplasm, hence, promoting its role as an electron transfer protein[3].

To fulfil its second equally important function in the initiation of apoptosis, Cyt c must acquire peroxidase activity in order to catalyse cardiolipin peroxidation that facilitates the release of Cyt c from mitochondria. Specifically, many experiments have shown that upon binding to CL, Cyt c acquires peroxidase activity[4] that leads to peroxidation of CL, detachment of Cyt c from the inner mitochondrial membrane, release into the cytosol and subsequent induction of apoptosis through caspase activation. To gain a better understanding of this complex process, the interaction of ferric Cyt c with mitochondrial CL has been studied extensively over the past decade. Three distinct sites on the Cyt c surface have been suggested to be possible regions of interaction with CL: the A site, formed by Lys72, Lys73, Lys86 and Lys87; the C site, located near Asn52;[5–8] and the L site involving Lys22, Lys 27, His33, Lys25 and His26, that operates at low pH.[9,10] Recently, a novel CL binding site, termed the N-site, centered on residues Phe36, Gly37, Thr58, Trp59, and Lys60 has been found by studying the Cyt c-CL interaction in reverse micelle encapsulation.[11] Surprisingly, unlike all the earlier studies of this interaction, the protein structure does not appear to be significantly disturbed by the binding of cardiolipin in the reverse micelle.[11]

The appearance of peroxidase activity in Cyt c has been attributed to the partial unfolding of the protein[10,12,13], consequent rupture of the bond between the heme iron and its axial ligand

Met80,[12,14–17] and formation of alternative non-native conformers. It is notable that such non-native conformers appear also able to induce reversible pore formation enabling translocation of Cyt c more readily across the inner mitochondrial membrane.[18] Moreover, a monoclonal antibody specific for a non-native form of mammalian Cyt c that recognizes the phospholipid-bound Cyt c and does not recognize native Cyt c has been shown to label mitochondria in cells at an early stage of apoptosis prior to the acquisition of characteristics that define the apoptotic state.[19] This indicates that a conformational change in Cyt c, likely indicative of the peroxidase-active conformation obtained through its association with cardiolipin, occurs not only *in vitro* but also in cells.

Although the interaction between Cyt c and CL has been extensively studied, there is still no overall consensus regarding the conformational rearrangements of Cyt c that follow the protein-lipid interaction. It has been proposed that the ferric Cyt c-CL complex contains a mixture of 5-coordinate high spin (5cHS),[10] 6-coordinate high-spin (6cHS)[10,16] and misligated 6-coordinate low spin (6cLS) species. There is also no consensus regarding the nature of the sixth endogenous low spin ligand, being identified as a Lys,[15,16,20] a His[10,17] or an OH^- ion.[15]

In the present work, to rationalize the different results and gain better insight into the Cyt c-CL interaction, we have studied the formation of the CL complex of the ferric horse heart wild type (WT) protein and selected mutants in which residues considered to play a key role in the interaction with CL (His26, His33, Lys72, Lys73, Lys79) have been mutated. The analysis was conducted at both room and low temperature via UV-vis absorption, resonance Raman (RR), and electron paramagnetic resonance (EPR) spectroscopies.

EXPERIMENTAL PROCEDURES

MATERIALS

Horse heart Cyt c (approximately 95% purity, lyophilized oxidized form) and cardiolipin, as sodium salt from bovine heart (approximately 98% purity, lyophilized powder), were obtained from Sigma-Aldrich (Steinheim, Germany) and used without further purification. All reagents were of analytical grade. Gaseous CO was purchased from Rivoira (Milan, Italy).

METHODS

Construction of the horse heart Cyt c expression system

A version of the horse heart Cyt c synthetic gene was designed on the basis of the sequence of a previously reported Cyt c synthetic gene[21] and its synthesis performed by Primm srl (Milano, Italy). A detailed description of the preparation of the expression system and mutation of the horse heart Cyt c expression construct has been published previously[22]. Note that the double and triple mutations were introduced by subsequent rounds of mutagenesis.

Cell growth and purification of recombinant proteins

The expression plasmids of horse heart Cyt c were introduced into *E. coli* JM 109 as wild type (WT) or its variants. Protein expression and purification of the recombinant protein were then conducted as previously described.[23]

Preparation of Cyt c-CL complexes

Lyophilized ferric Cyt c was dissolved in 20 mM Hepes at pH 7.0 and concentrated solutions of the Cyt c mutants were diluted with the same buffer. To ensure complete oxidation, 1-3 μL of a 3 mM freshly prepared $K_4[Fe(CN)_6]$ solution was added to 40 μL protein solutions.

The WT-CL complex was prepared following a previously reported procedure.[14] Briefly, CL was dissolved by sonication in ethanol, obtaining a 10 mM solution. The CL ethanol solution was then added to the WT protein and Cyt c mutants in order to obtain a Cyt c-CL molar ratio (R) of 1:30, corresponding to the final point of the CL titration (see below). To avoid any possible effect on the protein triggered by the ethanol used to dissolve CL, careful controls were made to ensure that no spectral changes were caused by the ethanol added to the protein. Figure S1 demonstrates that the addition of 3% ethanol does not affect the UV-Vis (panel A) and RR spectra (panel B) of WT Cyt c. In fact, the RR spectra (panel B) of WT Cyt c without ethanol (trace c) is identical to that obtained after subtraction of the 3% ethanol spectrum (trace b). The maximum amount of the CL ethanol solution added to Cyt c to form the Cyt c-CL complex corresponds to 3% ethanol v/v. It is noted that the maximum concentration of ethanol that does not cause spectral changes is 10% v/v (Figure S1, panel B, traces c and d). Hence, the level of ethanol added to the protein in this study (3%) is well below that expected to lead to spectral variations. As a consequence of limiting the ethanol concentration to 3%, the Cyt c concentration for a Cyt c-CL molar ratio of 1:30 cannot exceed 25 μM.

Ferrous samples and the CO complex were prepared as previously reported.[24]

Cyt c concentrations in the range 10–200 μM were used for WT samples, whereas concentrations in the range 20-25 μM were used for the Cyt c mutants and the Cyt c-CL complexes. The protein concentration was determined using an extinction coefficient (ε) of 106 mM^{-1} cm^{-1} at 409 nm.[25]

Preparation of model compounds

His-Fe-His (bis-His) model: ferric Cyt c was dissolved in 50 mM phosphate at pH 7.0 to obtain a 50 μM solution. Then 30 μL of a 75 mM SDS solution was added together with 90 μL of a 0.1 M imidazole solution, in order to obtain a sample with a final SDS concentration of at least 10 mM and an imidazole/Cyt c ratio of 2500:1.[26]

Lys-Fe-His model: ferric Cyt c was dissolved in 150 mM phosphate at pH 12.1 to achieve a final concentration in the range of 60-100 μM.

OH^--Fe-His model: 85 μL of Cyt c K727379N (horse heart Cyt c Lys72Asn/Lys73Asn/Lys79Asn triple mutant) in 20 mM Hepes at pH 7.0 were diluted with 15 μL of 150 mM phosphate at pH 12.1 to achieve a final concentration in the range of 25 μM at pH 12.0.

Note that to ensure complete oxidation of Cyt c in the His-Fe-His and Lys-Fe-His model compounds, 3 μL of a 3 mM freshly prepared $K_4[Fe(CN)_6]$ solution was added to 70 μL protein samples.

Electronic absorption measurements

Electronic absorption measurements were recorded using a 5 mm NMR tube (300 nm/min scan rate) or a 1 cm cuvette (600 nm/min scan rate) at 25°C by means of a Cary 60 spectrophotometer (Agilent Technologies) with a resolution of 1.5 nm. The spectrophotometric titration measurements were performed using a 1 cm path-length cuvette. All spectra were baseline-subtracted and corrected for the dilution factor. The spectra were differentiated applying the Savitzky–Golay method using 15 data points (LabCalc, Galactic Industries, Salem, NH). Both the wavelength and bandwidth were invariant when the number of points was increased or decreased. Absorption spectra were measured both prior and after RR measurements to ensure that no degradation occurred under the experimental conditions used.

Resonance Raman measurements

The resonance Raman spectra were obtained at 25°C using a 5 mm NMR tube by excitation with the 406.7 and 413.1 nm lines of a Kr^+ laser (Coherent, Innova 300 C, Coherent, Santa Clara, CA, USA) and with the 441.6 nm line of a He–Cd laser (Kimmon IK4121R-G). The RR spectra were recorded as previously reported.[24]

A spectral simulation program (LabCalc, Galactic Industries, Salem, NH, USA) using a Lorentzian line shape was used in order to determine peak positions, bandwidth and intensity. The frequencies of the bands were optimized to an accuracy of 1 cm^{-1} and the bandwidths 0.5 cm^{-1}. Bandwidths (full width at half-maximum) varied as follows: 12–15 cm^{-1} in the high-frequency region and 9–14 cm^{-1} in the low-frequency region.

Low temperature resonance Raman measurements

200-300 μL of the samples were put in a 1.5 cm diameter quartz crucible that was positioned in a THMS600 cryostat (Linkam Scientific Instruments, Surrey, UK) and frozen. After freezing the sample, the cryostat was positioned vertically in front of the spectrometer and the laser light was

directed onto the quartz window. To avoid sample denaturation and reduction of the ferric samples, the laser position was changed frequently and a cylindrical lens, which focuses the laser light into a line instead of a point, was used. The sample temperature was maintained at 80 K.

EPR measurements

EPR spectra were recorded with an Elexsys E500 (Bruker, Rheinstetten, Germany), equipped with an NMR gaussmeter and a microwave frequency counter. An ESR 900 cryostat (Oxford Instruments, Abingdon, UK), was used to obtain low temperatures. Spectra were acquired under non-saturating conditions using 1 mT modulation amplitude, the temperature and microwave power for each sample are reported in the figure captions. The g values were determined by careful visual inspection of the spectra.

RESULTS

Ferric form

In order to follow the conformational changes that are induced by the addition of CL, Cyt c has been titrated with CL. The experimental approach adopted in this study is based on the use of an ethanol solution of CL rather than the more commonly used mixture of liposomes. There are many studies in the literature that have revealed the complex nature of Cyt c binding to anionic lipids on surface membranes that is also dependent on the mixture of lipids that constitute the liposome together with CL,[9,12,27–30] which will be absent for CL binding in an ethanol solution. However, two recent studies, which compared the effects on the properties of the Cyt c-CL complex by using CL in an ethanol solution or liposomes constituted by CL/PC mixtures, have demonstrated that the model system used has negligible effect on the heme structure of the Cyt c-CL complex.[14,17] Therefore, the simpler model system used in the present study is considered to be a valid experimental approach that does not compromise the outcome of the study. Moreover, all the RR spectra reported in the manuscript were obtained using excitation wavelengths corresponding to the electronic absorption Soret band. Hence, the RR bands observed necessarily derive from the heme group; protein regions that are not in the proximity of the heme group will not be detected. Hence, the protein conformational state identified herein is considered a good representation of that found for the extended E-like states on liposomes proposed by Pletneva and coworkers.[12,28] The sequence of structural events that is prompted by the addition of CL has been monitored by electronic absorption, RR (at room temperature and 80 K), and EPR (Figure 1). The spectra of a His-Fe-His18 (bis-His) model compound are also reported for comparison. The model compound is obtained at pH 7.0 by adding imidazole to Cyt c in 10 mM SDS at an imidazole/Cyt c ratio of 2500:1.[26]

At a protein-lipid molar ratio (R) of 1:5 a number of differences compared to the WT protein are evident. The CT band at 695 nm decreases (Figure 1, A right), in the high frequency RR spectrum the ν_3 band at 1502 cm^{-1} and the ν_2 at 1584 cm^{-1} broaden (Figure 1, D) and in the low frequency region the band at 568 cm^{-1}, assigned to the out-of-plane mode, γ_{21}, slightly decreases in intensity

(Figure 1, C). Although the WT species remains predominant, the spectral changes indicate an initial rupture of the Fe-Met80 bond and the formation of a new 6-coordinate low spin (6cLS) species where the distal Met80 ligand has been replaced by another residue.

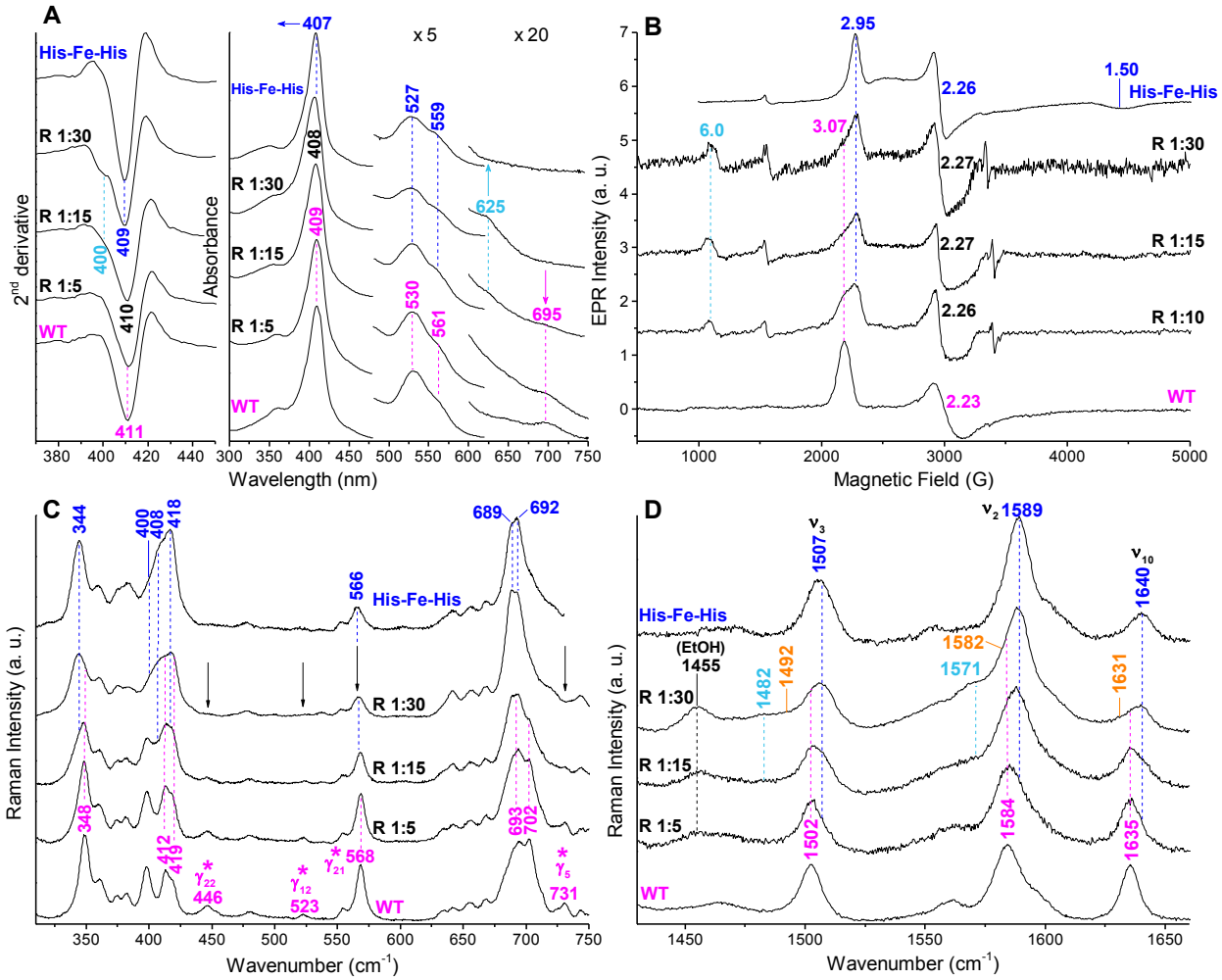

Figure 1. Titration of WT Cyt c with CL followed by UV-Vis, EPR and RR spectra. UV-Vis and second derivative spectra (panel A), EPR spectra (panel B) and RR spectra in the low (panel C) and high (panel D) frequency regions of the WT protein and the R 1:5 (R 1:10 in panel B), R 1:15, R 1:30 WT-CL complexes in 20 mM Hepes at pH 7.0, 298 K. The spectra of the bis-His model are also shown for comparison. The band positions (wavelengths, frequencies, g-values) due to the His-Fe-Met native species, the His-Fe-His species, the 6cHS and the 5cHS species are shown in magenta, blue, light blue and orange, respectively. The spectra have been shifted along the ordinate axis to allow better visualization. In panel A the 470–620 nm and the 600–750 nm regions of the

spectra are expanded 5-fold and 20-fold, respectively. In panels C and D the intensity of the spectra is normalized to that of the ν_4 band. EPR experimental conditions: **WT protein**: 190 μM, 10 K, microwave power 0.53 mW; **R 1:10** 75 μM, 5 K, microwave power 8.3 mW; **R 1:15** 50 μM, 5 K, microwave power 8.3 mW; **R 1:30**: 25 μM, 5 K, microwave power 8.3 mW; **His-Fe-His**: 255 μM, 5 K, microwave power 8.3 mW. The spectra shown are after subtraction of the cavity signal. RR experimental conditions: excitation wavelength 406.7 nm, laser power at the sample 5 mW; **WT**: average of 4 spectra with 20 min integration time (C) and average of 5 spectra with 25 min integration time (D); **R 1:5**: average of 10 spectra with 50 min integration time (C) and average of 12 spectra with 60 min integration time (D); **R 1:15**: average of 6 spectra with 30 min integration time (C) and average of 4 spectra with 20 min integration time (D); **R 1:30**: average of 12 spectra with 60 min integration time (C) and average of 21 spectra with 105 min integration time (D); **His-Fe-His**: laser power at the sample 10 mW, average of 12 spectra with 60 min integration time (C) and average of 10 spectra with 50 min integration time (D).

The asterisks (*) in panel C indicate the out-of-plane modes.

At a protein-lipid molar ratio of 1:15 the changes become more pronounced, characterized by a slight blue-shift of the Soret band, a further decrease in intensity of the band at 695 nm (Figure 1, A right), the appearance of distinct shoulders at 1507 and 1589 cm^{-1} in the high frequency RR spectrum (Figure 1, D), and a marked intensity decrease of all the out-of-plane modes: γ_{22} (446 cm^{-1}), γ_{12} (523 cm^{-1}), γ_{21} (568 cm^{-1}), and γ_5 (731 cm^{-1}) (Figure 1, C). Moreover, a new CT band at 625 nm is observed in the UV-Vis spectrum (Figure 1, A right), together with a new Soret band centred at 400 nm in the second derivative spectrum (Figure 1, A left). In the RR spectrum, weak bands at 1482 and 1571 cm^{-1} (Figure 1, D) reveal the presence of a 6cHS (aquo) species. The EPR spectra (for R 1:10 and 1:15) confirm the presence of a HS form (g = 6.0), together with a new 6cLS species [g = 2.95, 2.27] and that of WT Cyt c [g = 3.07, 2.23, 1.25][31] (Figure 1, B); the g_3 value of the former species is too weak to be observed. It should be noted that the poor quality of the EPR

spectra of the CL complexes is due to the obligate use of very dilute samples (< 25 μM), necessary to maintain the level of ethanol (required to solubilize CL) below that resulting in protein denaturation, and the presence of several spin species. This leads to the consequent difficulties of achieving a good subtraction of the cavity signal at g ~ 2 (ca. 3300 G), which deforms the resultant spectrum in this region.

Upon increasing further the molar ratio, the 6cHS and the new 6cLS species further increase at the expense of the native form. At the final protein-lipid molar ratio of 1:30 (no further changes are observed for R > 1:30), all the techniques (UV-Vis, RR and EPR) clearly indicate that the predominant form is a misligated 6cLS species, together with a minor non-ligated 6cLS WT form.

Moreover, a detailed curve-fitting analysis of the RR spectrum at room temperature revealed the presence of two high spin species (6cHS: ν_3 1482 cm^{-1}, ν_2 1571 cm^{-1} and 5cHS: ν_3 1492 cm^{-1}, ν_2 1582 cm^{-1}, ν_{10} 1631 cm^{-1}). In order to confirm the data analysis, we have also carried out the spectral decomposition at low temperature, which benefits from a narrowing of the bands. However, only the 6cLS is observed in the RR spectrum at low temperature (Figure S2). Interestingly, the high spin form is still present in the EPR spectrum as a minor species (g = 6.0, Figure 1, B). This apparent difference in properties noted between the two techniques is possibly ascribable to a slower freezing rate for the Raman experiments.

Importantly, by subtracting the ethanol band from the high frequency room temperature RR spectrum of Cyt c + CL (Figure S3, spectrum b), the frequency changes of the Cyt c bands induced by CL (Figure 1, D; Figure S3, spectrum c), are confirmed. It is noted that to avoid perturbing the curve-fitting analysis of the RR spectrum (Figure S2), the spectrum without subtraction of the ethanol band was used.

The spectroscopic markers of the misligated 6cLS form are: i) a Soret band blue-shifted (407 nm) with respect to the WT protein (409 nm) (Figure 1, A); ii) core size marker bands at 1507 (ν_3), 1589 (ν_2), and 1640 (ν_{10}) cm^{-1} (Figure 1, D), up-shifted with respect to the WT (ν_3 1502 cm^{-1}, ν_2 1584

cm^{-1}, ν_{10} 1635 cm^{-1}); iii) very weak or absent RR bands corresponding to the out-of-plane modes (Figure 1, C), indicating a loss of the heme distortion typical of the WT protein; iv) new bands at 343 cm^{-1} (ν_8) and at 400 cm^{-1}; v) intensity increase of the $\delta(C_\beta C_A C_B)$ band at 419 cm^{-1}; vi) EPR g values at g_1 = 2.95 and g_2 2.27 (Figure 1, B). All these spectroscopic markers correspond to the 6cLS bis-His species observed in the bis-His (imidazole bound) Cyt c model compound (indicated in blue in Figure 1).[26,31–33] Therefore, in agreement with recent findings,[17] this new species is attributed to a 6cLS bis-His species in which the Met80 residue has been replaced by His26 or His33 (His18-Fe-His26/His33). This clearly results from a global rearrangement of the protein, since neither His26 nor His33 are located in proximity of the heme iron. Accordingly, the new RR band at 400 cm^{-1} is assigned to the ν_{AS}(Fe-Im_2) mode, as previously observed in the spectra of Cyt c-CL[17], Lys72/73Asn/His26Tyr-CL complex,[22] of the bis-His coordinated N-fragment of Cyt c,[32] as as well in imidazole and imidazolate complexes of microperoxidase.[34] The corresponding ν_S(Fe-Im_2) mode[34,35] is assigned to the band observed at 206 cm^{-1} only in the spectra of the bis-His model compound and the Cyt c-CL complex (molar ratio of 1:30) (see below, Figure 3, A).

In order to confirm the presence of a bis-His complex and possibly identify the His residue bound to the heme Fe in the misligated Cyt c-CL complex, we have studied the CL complex for selected mutants; namely, those involving the His26, His33, Lys72, Lys73, and Lys79 residues. The unligated forms of these mutants have been previously studied. It has been shown that the triple mutations have only a minor effect on the WT protein and in particular that the mutations have little effect on the local heme structure.[22]

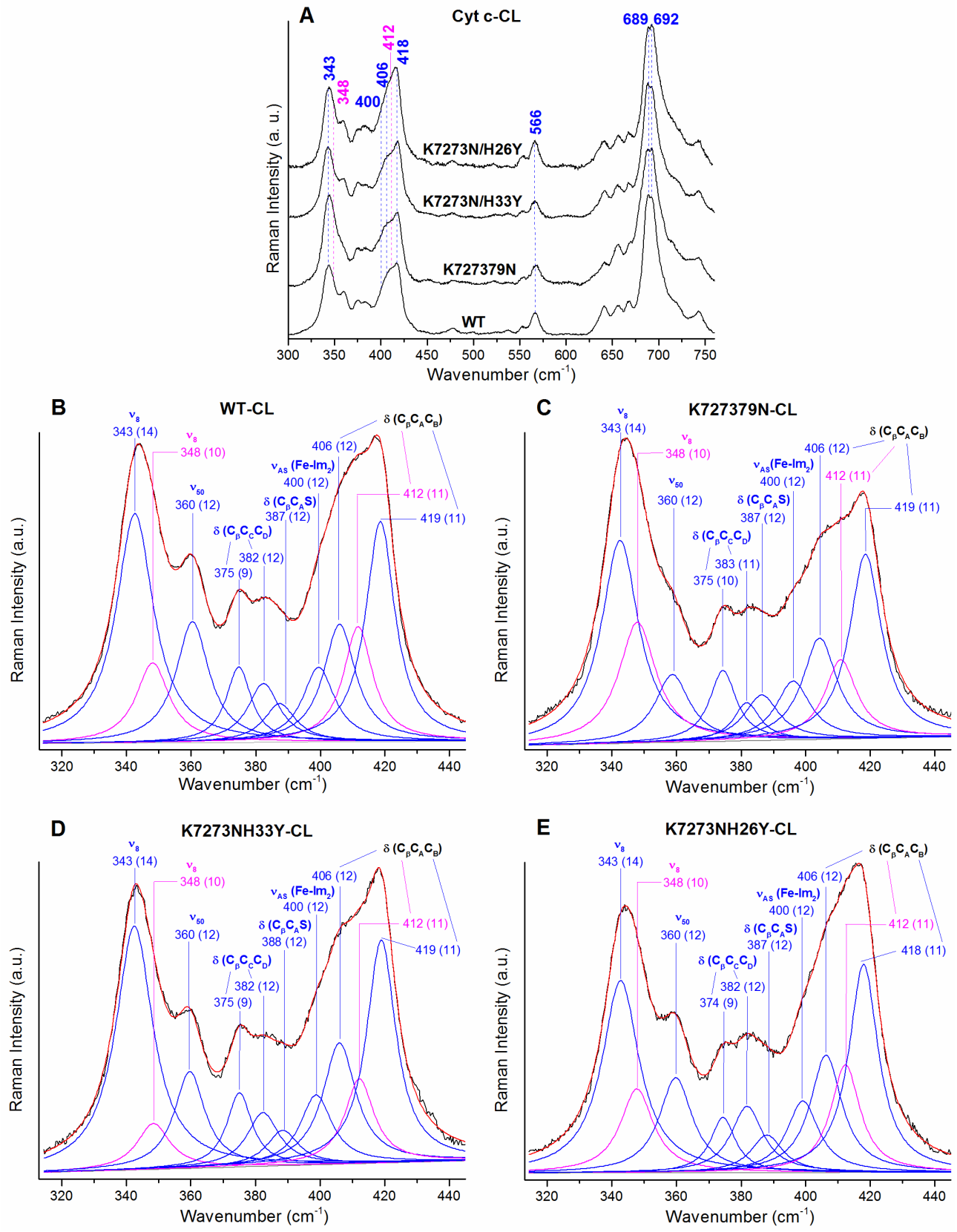

Figure 2. RR spectra in the low frequency region at 298 K together with the curvefitting analysis of the R 1:30 CL complexes of the WT protein and selected mutants. RR spectra at 298 K (panel A) and the curvefitting analysis (panels B, C, D, E) of the low frequency region of the

R 1:30 CL complexes of the WT protein (B) and of the Cyt c K727379N (C), K7273N/H33Y (D), K7273N/H26Y (E) mutants. The frequencies of the bands due to the 6cLS His-Fe-Met native species and of the 6cLS bis-His species are shown in magenta and blue, respectively. The spectra have been shifted along the ordinate axis to allow better visualization and the intensity of the spectra is normalized to that of the ν_4 band. Experimental conditions: 20 mM Hepes pH 7.0, excitation wavelength 406.7 nm, laser power at the sample 5 mW; average of 12 spectra with 60 min integration time (WT), average of 18 spectra with 90 min integration time (K727379N), average of 20 spectra with 100 min integration time (K7273N/H33Y), average of 18 spectra with 90 min integration time (K7273N/H26Y).

Figure 2, A shows the low frequency region RR spectra of the CL complexes of the triple mutants K727379N, K7273N/H26Y (horse heart Cyt c Lys72Asn/Lys73Asn/His26Tyr triple mutant), and K7273N/H33Y (horse heart Cyt c Lys72Asn/Lys73Asn/His33Tyr triple mutant) compared with that of WT Cyt c. The corresponding high frequency region RR spectra are shown in Figure S4. The K727379N-CL mutant binds CL giving rise to a CL complex very similar to that of the WT protein. In fact, the curvefit analysis (Figure 2, B and C) shows that the CL complex of the WT and K727379N mutant can be fitted with the same parameters (same number of bands with the same frequencies and bandwidths). The richness of the RR spectra of Cyt c is associated with heme protein interactions in the native structure, i.e. a dominant ruffling distortion of the heme group.[36,37] It is noted that the band frequencies used in the curvefitted spectra correspond well to those reported in the literature for the same Raman modes of Cyt c and model compounds.[26,32,34,38–40] The slight differences that can be observed by visual inspection depend on the different amounts of unligated protein that remains after complexation (ν_8 at 348 cm^{-1} and ($\delta(C_\beta C_a C_b)$ at 412 cm^{-1}). Therefore, any involvement of the Lys residues in heme iron coordination in the WT-CL complex can be completely excluded. Interestingly, the CL complexes of both K7273N/H33Y and K7273N/H26Y are characterized by a predominant 6cLS bis-His species. Furthermore, as shown by the curvefit of

the spectra (Figure 2, D and E), once again they differ only in the amount of unligated WT protein which remains after complexation. This finding clearly indicates that both histidines are capable of replacing Met80 in the WT-CL complex, as previously observed for the interaction between Cyt c and CL liposomes.[22]

To confirm that an endogenous His is involved in the formation of the misligated species of the CL complex, we have studied the double H2633N mutant (horse heart Cyt c His26Asn/His33Asn double mutant). UV-Vis and RR spectra demonstrate that the mutation does not alter the protein significantly (Figure S5).

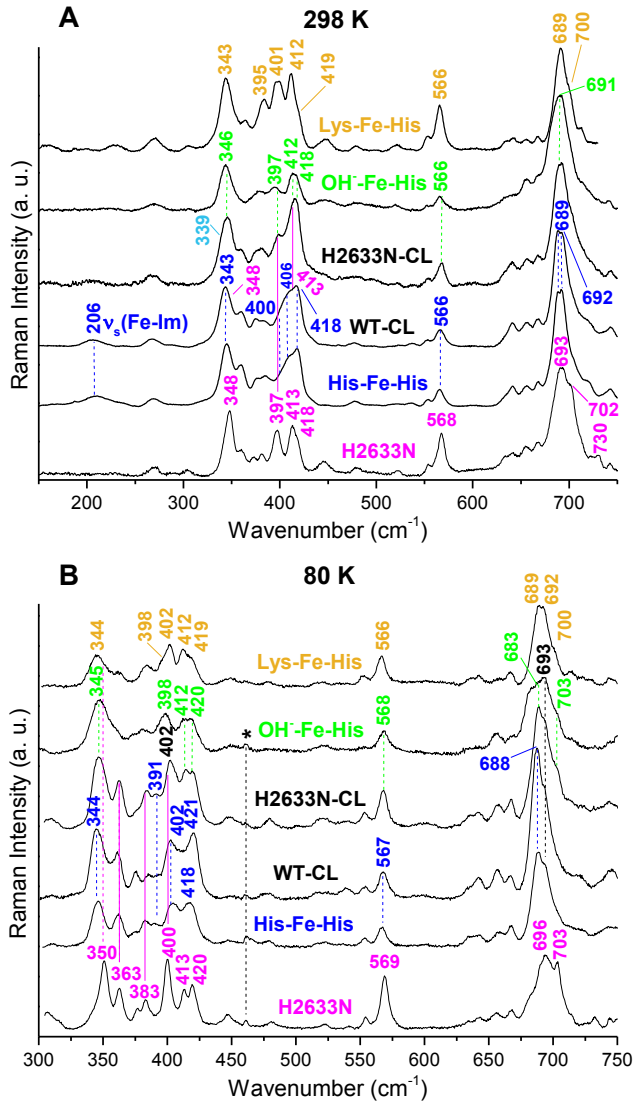

Figure 3. RR spectra at 298 K (panel A) and at 80 K (panel B) in the low frequency region of the H2633N mutant and the CL-complexes of the WT protein and the H2633N mutant. The

spectra of the bis-His, OH^--Fe-His, and Lys-Fe-His models are also shown for comparison. The frequencies of the bands assigned to the Met-Fe-His native species, the His-Fe-His species, the OH^--Fe-His species and the Lys-Fe-His species are shown in magenta, blue, green and light brown, respectively. The spectra have been shifted along the ordinate axis to allow better visualization and the intensity of the spectra is normalized to that of the ν_4 band. The spectra at 298 K were obtained using a spherical lens while those at 80 K were obtained using a cylindrical lens. Experimental conditions: excitation wavelength 406.7 nm, laser power at the sample 5-10 mW; **H2633N**: average of 18 spectra with 90 min integration time (A) and average of 30 spectra with 60 min integration time (B); **His-Fe-His**: average of 12 spectra with 60 min integration time (A) and average of 29 spectra with 145 min integration time (B); **WT-CL** (R 1:30): average of 12 spectra with 60 min integration time (A) and average of 11 spectra with 55 min integration time (B); **H2633N-CL** (R 1:30): average of 24 spectra with 120 min integration time (A) and average of 40 spectra with 80 min integration time (B); **OH^--Fe-His**: average of 11 spectra with 55 min integration time (A) and average of 27 spectra with 54 min integration time (B); **Lys-Fe-His**: average of 11 spectra with 55 min integration time (A) and average of 20 spectra with 10 min integration time (B).

Figure 3 shows the low frequency RR spectra at room temperature (A) and 80 K (B) of H2633N and its CL complex, together with different model compounds that represent possible heme coordination states (OH^--Fe-His, Lys-Fe-His, and His-Fe-His), and the WT-CL complex. The RR spectrum of the H2633N-CL complex, which is similar to that previously reported,[17] is markedly different from that of the corresponding WT-CL complex. Interestingly, it has striking similarities with that of the OH^- model compound (K727379N mutant at pH 12, identical to the yeast iso-1-Cyt c at pH > 10.5[38]). Therefore, the low-frequency region between 300 and 450 cm^{-1} confirms the identification of a hydroxide as the sixth ligand in the H2633N-CL complex. A specific spectral marker for the replacement of the Met ligand with a hydroxide ion is the significant loss of intensity of the prominent band at 397 cm^{-1}. The bands at 397 and 413 cm^{-1} of the unligated H2633N are

responsible for the different relative intensities observed in this region in the spectrum of the complex compared to that of the Fe-OH^- model compound at room temperature. At low temperature the bands at 363, 383 and 400 cm^{-1} of unligated H2633N overlap with those of the complex. The band at 339 cm^{-1} in the room temperature spectrum is assigned to the ν_8 mode of the HS components, which in this complex appears to be more abundant than in the WT-CL complex, as suggested by the ν_3 modes at 1482 (6cHS) and 1492 (5cHS) cm^{-1} in the RR high frequency region (Figure S2), the blue-shift of the Soret band to 404 nm and the CT band at 625 nm (Figure S6).

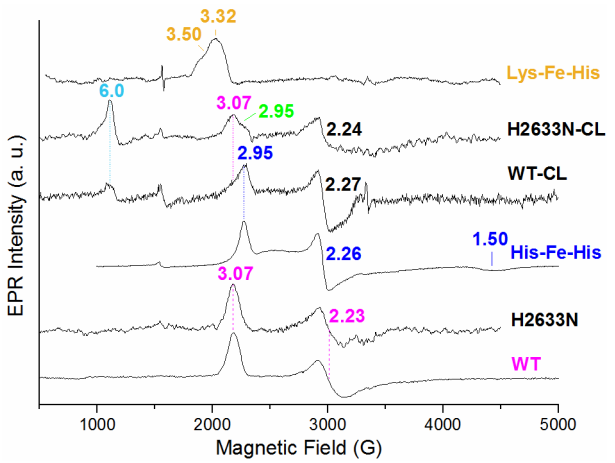

Figure 4. EPR spectra of the WT protein, the H2633N mutant and their CL-complexes in 20 mM Hepes pH 7.0. The spectra of the bis-His and Lys-Fe-His models are also shown for comparison. The g-values of the bands assigned to the Met-Fe-His native species, the His-Fe-His species, the Lys-Fe-His and the 6cHS species are shown in magenta, blue, light brown, and light blue, respectively. The spectra shown are after subtraction of the cavity signal and have been shifted along the ordinate axis to allow better visualization. Experimental conditions: **WT protein**: 190 μM 10 K, microwave power 0.53 mW; **H2633N mutant**: 50 μM, 15 K, microwave power 4.2 mW; **His-Fe-His**: 255 μM, 5 K, microwave power 8.3 mW; **WT-CL** (R 1:30): 25 μM 5 K, microwave power 8.3 mW; **H2633N-CL** (R 1:30): 25 μM, 15 K, microwave power 4.2 mW; **Lys-Fe-His**: 150 μM 15 K, microwave power 4.2 mW. In order to minimize accumulation times, some spectra were recorded for a reduced sweep width.

The presence of a hydroxo ligand in the sixth coordination position of the heme Fe in the H2633N-CL complex contradicts the previous assignment of the misligated form to a Lys-His coordination[17]. In order to confirm the nature of the sixth ligand we recorded the EPR spectra of the mutant and its CL complex (Figure 4), since Lys-Fe-His heme species may give rise to g_1 features near 3.5 and 3.3 whereas OH^--Fe-His species differ markedly, giving rise typically to features at g values similar to those observed for the alkaline form of myoglobin (Mb) (2.55, 2.17, 1.85).[31,33,41] The EPR spectra of model compounds characterized by His-Fe-Lys and His-Fe-His coordination, and the WT-CL complex are also shown. Unfortunately, all attempts to obtain the EPR spectrum of the K727379N mutant at pH 12 (OH^- model compound) by applying various conditions of temperature and microwave power failed. The reason for this is unclear; however, the low sample concentration imposed by the impossibility to achieve a sufficiently high yield of protein to prepare a concentrated sample may certainly be a factor. The EPR spectrum of the H2633N-CL complex indicates the presence of a mixture of 6cHS (g = 6.0), Met-Fe-His LS as for WT (g_1 = 3.07), and a species with g_1 = 2.95, which is accidentally identical to the g_1 value of the bis-His species. In the absence of the only two His residues (His26 and His33) that are able to bind the heme Fe, the most likely interpretation of the g_1 = 2.95 signal is a OH^--Fe-His species where the OH^- ligand is strongly H-bonded, as reported for HRPC and HRPA2 at alkaline pH.[42,43]

Ferrous form

The study of the CL complex has been extended to the ferrous form and its adduct with CO. These species do not have any functional relevance, but their RR spectra can give information on the status of the proximal Fe-His bond and the distal cavity, respectively. In fact, the complexation between Cyt c and CL has been reported to increase the 5cHS species in the ferrous form that, therefore, binds the CO ligand.[14]

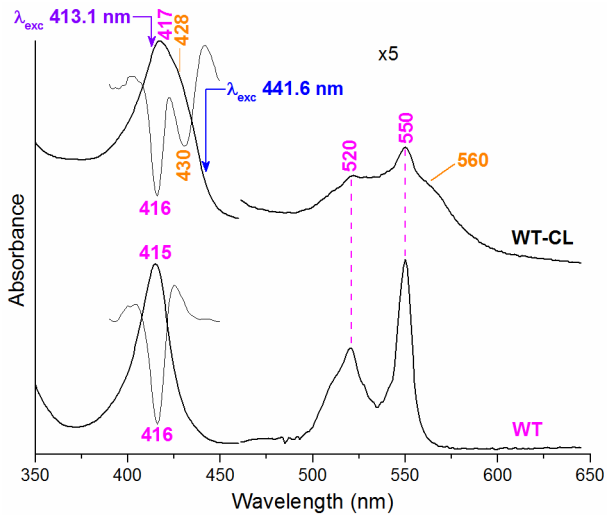

Figure 5. UV-vis spectra of the ferrous WT protein and the WT-CL R 1:30 complex. The wavelengths of the bands assigned to the His-Fe-Met native species and the 5cHS species are shown in magenta and orange, respectively, and the two excitation laser lines at 413.1 nm and 441.6 nm are shown in violet and blue, respectively. The 470–650 nm region of the spectra is expanded 5-fold. The spectra have been shifted along the ordinate axis to allow better visualization.

As previously reported,[14] on addition of sodium dithionite to the ferric WT-CL complex the ferrous WT-CL derivative is formed and its absorption spectrum (Figure 5) is characteristic of a 5cHS form (428 and 560 nm) in equilibrium with the 6cLS WT protein, as clearly indicated by the second derivative spectra in the Soret region. Therefore, upon reduction, a certain amount of CL detaches from Cyt c. The corresponding RR spectra in the high (Figure S7) and low frequency regions (Figure 6) confirm the presence of these two forms, the 5cHS being enhanced for 441.6 nm excitation, i.e. in resonance with the 5cHS Soret band. Accordingly, it has been recently reported that, although interaction of ferrous Cyt c with CL under aerobic conditions at high cardiolipin concentrations leads to oxidation of the protein and protein unfolding, the effects are significantly less than for the ferric state.[44]

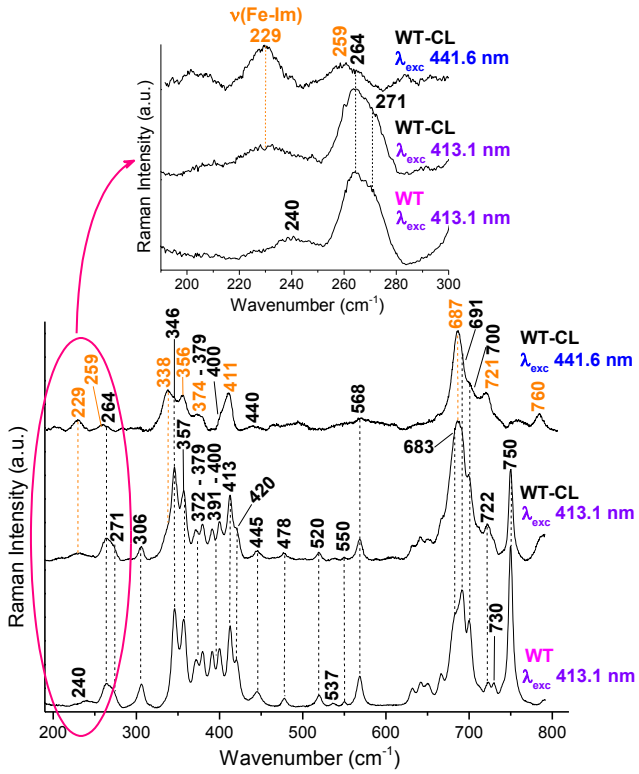

Figure 6. RR spectra at 298 K in the low frequency region of the ferrous WT protein (λ_{exc} 413.1 nm) and the WT-CL R 1:30 complex (λ_{exc} 413.1 nm and λ_{exc} 441.6 nm). The frequencies of the bands assigned to the 5cHS species are shown in orange. The spectra have been shifted along the ordinate axis to allow better visualization and the intensity of the spectra is normalized to that of the ν_4 band. Experimental conditions: **WT**: excitation wavelength 413.1 nm, laser power at the sample 5 mW, average of 4 spectra with 20 min integration time; **WT-CL**: laser power at the sample 6 mW, average of 15 spectra with 75 min integration time (λ_{exc} 413.1 nm) and laser power at the sample 26 mW, average of 15 spectra with 75 min integration time (λ_{exc} 441.6 nm). The **inset** shows the 190-300 cm^{-1} region expanded and the ν(Fe-Im) mode.

Previously, the 6cLS ferrous form had been assigned to a Lys-Fe-His species.[15] However, there are no RR data available in the literature for such a species to be able to support this hypothesis.[45]

In the low frequency region (Figure 6), the comparison between the RR spectra of the reduced complex for excitation at 413.1 nm, in resonance with the 6cLS species, and at 441.6 nm, in

resonance with the 5cHS species, enabled identification of the ν(Fe-His_{18}) stretching mode at 229 cm^{-1}, which is strongly enhanced for 441.6 nm excitation. The Fe–His bond stretching mode, is an optimum probe of the proximal cavity structure as it is very sensitive to the protein matrix, its frequency being strongly affected by the H-bonds between the N_δ atom of the proximal His and nearby residues.[46–48]

In the case of a neutral proximal His, the ν(Fe–His) mode has been found at around 200 cm^{-1}, while deprotonation at the N_δ position increases the frequency to 240 - 260 cm^{-1}. In myoglobin, where the N_δ proton is H-bonded to a neutral backbone carbonyl group, the ν(Fe–His) stretch is found at 220 cm^{-1}.[49] The frequency of the ν(Fe-His_{18}) band in the WT-CL complex is fairly high (229 cm^{-1}), suggesting that the bond between the heme iron and the N_ε of the proximal His18 is strong. Hence, we suggest that the His18 N_δ hydrogen is involved in the formation of a strong hydrogen bond with an accepting group. In analogy with previous work[32] and on the basis of the X-ray structure of Cyt c,[50] a good candidate as a hydrogen bond acceptor group is the oxygen of the carbonyl group of Pro30 at 2.7 Å from His18.

Ferrous-CO

The 5cHS ferrous species of the WT-CL complex binds CO, giving rise to a 6cLS complex with bands at 415, 532 and 562 nm in equilibrium with the ferrous WT protein (Figure S8).

The CO adduct has been used extensively as a probe of the nature and architecture of the heme-binding pocket. As the FeCO back-bonding is modulated by polar interactions and, in particular, by the formation of H-bonds between the bound CO and the distal protein residues,[51] the electrostatic interaction between the FeCO unit and the protein alters the electron distribution in the FeCO unit with the consequent change of the order of the C–O bond. An inverse linear correlation has been established between the frequencies of the ν(FeC) and ν(CO) stretching modes for a large class of heme protein CO complexes containing imidazole as the fifth iron ligand, the most common proximal ligand in heme proteins.[52] The ν(FeC)/ν(CO) position along the correlation line reflects

the type and strength of distal polar interactions,[51] as clearly shown by the CO adducts of several Mbs characterized by different distal interactions with the CO.[53]

The RR modes of the WT-CL CO complex have been identified at 491 cm^{-1} [ν(Fe-C)] and 1966 cm^{-1} [ν(CO)] (Figure 7). The ν(FeC)/ν(CO) position along the correlation line is very close to that obtained for the SW Mb mutant where an apolar residue (Val) replaces the polar distal His. Therefore, the WT-CL CO complex is characteristic of an upright conformation with no polar distal interactions, *i.e.* an open form.

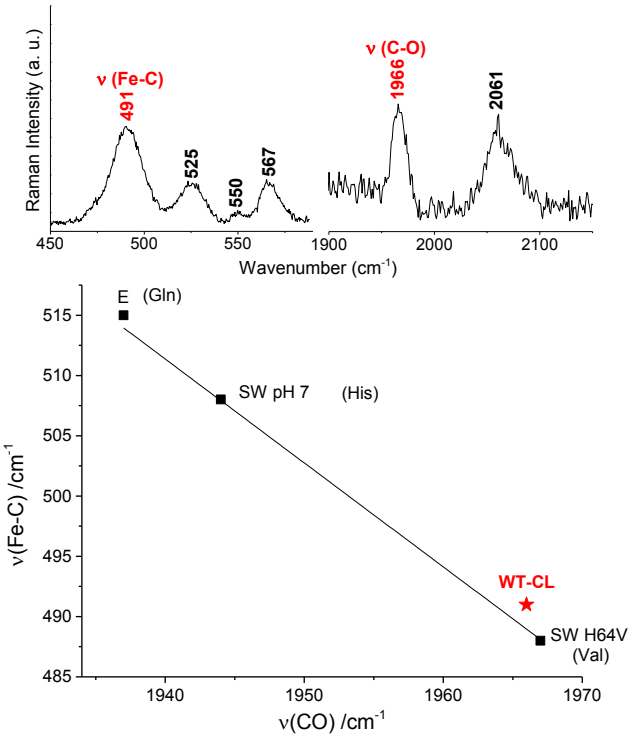

Protein	ν(Fe-C)	ν(C-O)
E: Elephant Mb	515	1937
SW: Sperm Whale Mb pH 7	508	1944
WT-CL	**491**	**1966**
H64V mutant of SW Mb	488	1967

Figure 7. WT-CL (R 1:30) complex CO adduct. (Top) RR spectra of the ferrous WT-CL CO adduct in the low and high frequency regions. The ν(Fe-C) and ν(C-O) frequencies are shown in red. (Bottom) back-bonding correlation plot for the ν(Fe-C) and ν(C-O) stretching frequencies of various myoglobins: E, elephant; SW pH 7.0, sperm whale at pH 7.0; SW H64V, sperm whale mutant where His64 has been substituted with a Val. The interpolation point of the ν(Fe-C) and

ν(C-O) frequencies of the WT-CL R 1:30 CO adduct is shown as a red star. The frequencies of the various CO adducts are reported in the table.

DISCUSSION

Cyt c binding to CL has been studied extensively using various experimental techniques, but a clear and reliable description of the interaction is still lacking. The 'Extended CL anchorage' model of CL interaction with Cyt c assumes that it is able to interact with the protein at two separate binding sites termed the A- and C-sites.[5] The A-site most likely involves weak electrostatic interactions between the phosphate groups of CL and lysine residues of Cyt c, whereas the C-site involves hydrophobic interactions and hydrogen bonding between one of the protonated, uncharged, phosphate groups of CL and the Asn52 residue. It has been suggested that one of the acyl chains of CL fits into a pocket of Cyt c, while the other three acyl chains remain in the membrane.[7,54] An alternative hypothesis suggests an interaction of two fatty acyls of CL with Cyt c.[8] However, recently, Pletneva and coworkers performed fluorescence energy transfer and biolayer interferometer experiments. The results suggest that, rather than the presence of two binding sites, there is an equilibrium between two conformations of Cyt c bound to cardiolipin containing liposomes , one with a globular structure (compact, C) and another with a more extended conformation (E). They claimed to have found no evidence for acyl chain insertion into the Cyt c interior.[12,28] Pandiscia and Schweitzer-Stenner[30] also studied the interaction between liposomes and Cyt c using a combination of fluorescence, visible circular dichroism and absorption spectroscopy. They obtained binding isotherms that are consistent with a one-site model and a conformational equilibrium between native-like and non-native-like conformations of the protein, the equilibrium depending on the protein density on the liposome surface. These results are highly reminiscent of the C ⇋ E equilibrium proposed by Pletneva and coworkers.[28]

All the experiments have established that protein binding to CL-containing membranes promotes partial Cyt c unfolding, changes of the Met80-heme iron interaction, and dramatically enhances the

peroxidase activity of the protein. However, while it is clear that the Met80 ligand is displaced upon CL binding, a unique consensus regarding the structure of the subsequently formed misligated protein is still lacking. Furthermore, the exact nature of the order of events that characterize the conformational rearrangements associated with Met80 replacement remains an open question.

In the present work, we have followed the structural changes induced in Cyt c by progressive additions of CL using electronic absorption, RR, and EPR spectroscopies. Moreover, the misligated species has been unequivocally identified by studying selected mutants, in which residues able to replace Met80 following interaction with CL (i.e. His26, His33, Lys72, Lys73, Lys79) have been mutated, together with model compounds of Cyt c, in which the sixth endogenous/exogenous ligand is a Lys, a His or an OH^- ion.

The titration of Cyt c with CL shows that partial Met80 detachment is observed at very low CL concentration (Cyt c:CL molar ratio of 1:5) and the spectroscopic data clearly indicate that the native ligand is replaced at this phase by a His, as the misligated form is unambiguously assigned to a 6cLS bis-His species, in agreement with a recent report.[17] As the CL concentration increases, the proportion of the bis-His species increases at the expense of the native Met80-Fe-His18 form which, however, remains in a small amount up to the end of the titration. Since neither His26 nor His33 are located in proximity of the heme iron (Figure 8), the formation of a bis-His species indicates that the extent of the protein rearrangement is long ranging, leading to a more flexible heme structure than in the WT protein. Moreover, the formation of a 6cHS (H_2O-Fe-His18, aquo) species, observed at molar ratios greater than 1:5, and a 5cHS (Fe-His18) species at the end of the titration, probably indicates some degree of lability of the misligated distal His, as suggested recently,[17] and reflects a further increase of protein flexibility. This finding is supported also by the RR spectrum of the CO-adduct, characterized by ν(FeC) and ν(CO) stretching mode frequencies very similar to those of the Mb mutant where an apolar residue (Val) replaces the polar distal His; hence, typical of an open form. The Raman stretching mode frequencies are consistent with a CO molecule that adopts an upright conformation with no polar distal interactions. On the contrary, the fairly high frequency of

the ν(Fe-His18) stretching mode (229 cm^{-1}) observed in the 5cHS ferrous form suggests the presence of a hydrogen bond between the N_{δ}(His18) hydrogen and an accepting group, consistent with a closed proximal cavity.

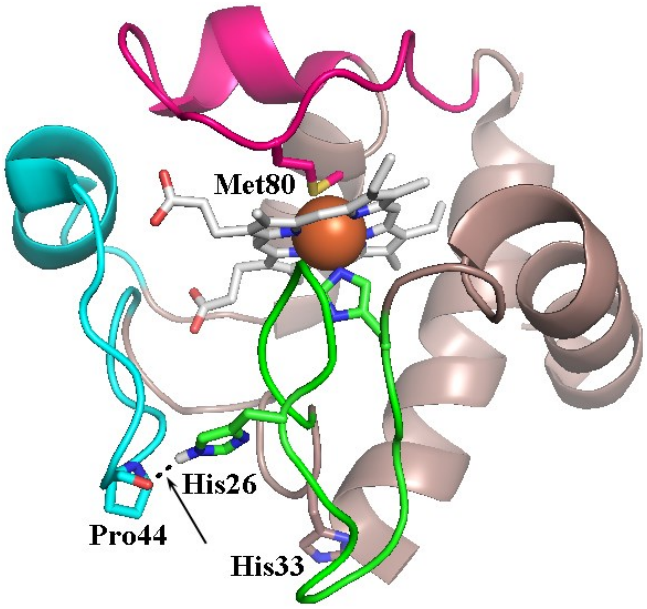

Figure 8. Ribbon diagram of the Cyt c structure. The figure highlights the Met80-containing loop (magenta), the 40s Ω loop (cyan), and the 20s Ω loop (green). The arrow highlights the His26-Pro44 H-bond (dotted line). This figure has been generated using the horse heart Cyt c three-dimensional structure deposited in the Protein Data Bank as entry 1HRC [37], prepared with PyMOL (http://www.pymol.org).

As recently suggested,[55] a highly plausible scenario that is able to explain the observed sequence of events that follows CL binding to Cyt c is focused on the breakage of the His26-Pro44 hydrogen bond, which bridges the 20s (residues 18-31) and the 40s Ω–loop (residues 40-57, highly conserved in class I Cytochromes) in the polypeptide chain.[50] This hydrogen bond, which links the 20s and 40s Ω–loops maintaining them sterically close (Figure 8), promotes a shielding effect of the 40s loop on the bottom heme edge and stabilizes the protein tertiary structure. Accordingly, a number of studies have reported that disruption of the His26−Pro44 hydrogen bond has considerable impact on the native protein conformation.[22,23,32,55–57] Moreover, the 40s Ω–loop , characterized as the least

stable cooperative unfolding unit ('foldon') in Cyt c,[58] is strongly destabilized at low pH. This effect has been attributed to the rupture of the H-bond between His26 and Pro44 as a consequence of protonation of His26, consistent with the observed increase in the His26 pKa.[55]

It is important to note that as the heme propionate substituents accept H-bonds from residues in the 40s Ω–loop, the conformational changes associated with its destabilization would be expected to modify the heme interactions with the protein matrix and, subsequently, prompt dissociation of the Met80 ligand. Accordingly, mutation of His26,[23] as well as excision of the 40s Ω–loop in the non-covalent complex reconstituted upon mixing two non-contiguous fragments of horse Cyt c (1–38/57–104 fragment complex),[56] significantly destabilizes the Cyt c structure with consequent marked impact on the heme pocket conformation and weakening of the Met80–Fe(III) axial bond strength. However, unlike in the presence of CL, the rupture of the His26−Pro44 hydrogen bond upon mutation of the His26 or excision of the 40s Ω–loop, gives rise to the formation of a Lys-Fe-His misligated species.

On the basis of our analysis, we can unequivocally rule out any involvement of a Lys residue, as previously suggested[15,16,20] or an OH^{-}[15] in the heme misligation induced by interaction with CL, which instead leads to ONLY His ligation. Furthermore, both His26 and His33 are capable of replacing Met80, in agreement with the results reported previously for the interaction between Cyt c and CL liposomes.[22]

As mentioned above, time-resolved FRET measurements revealed the presence of a conformational heterogeneity of the CL-bound Cyt c ensemble in which the diverse conformations are characterized by a clearly different extent of protein unfolding.[12,28] Interestingly, the variations induced in the Cyt c structure upon interaction with CL recall the protein folding mechanism in solution. In fact, a fraction of the ensemble is substantially unfolded, resembling the guanidine hydrochloride-denatured state. In this state, in conditions of highly concentrated urea or GdnHCl solutions, the His-Fe-His ligation has also been observed.[59–63] Based on these results, Russell[59] suggested that non-native His ligation in unfolded Cyt c plays an important role in determining

protein stability and dynamics. To date, studies on Cyt c indicate that a potential non-native His ligand is present in the majority of mitochondrial Cyts c,[64] suggesting that non-native His ligation upon unfolding may have evolved to serve a specific function in mitochondrial Cyts c.

The present results have resolved a longstanding debate about the nature of the structural changes of cytochrome c, induced by cardiolipin, in the pre-apoptotic process. In fact, we show that when the Cyt c-CL interaction is complete, a major misligated bis-His species is formed, together with minor contributions of 6cHS and 5cHS species, which coexist with a small residue of the native protein. The formation of the bis-His species is likely triggered by the rupture of the His26-Pro44 hydrogen bond, which leads to the destabilization of the 40s Ω-loop, and resembles the unfolding mechanism observed in solution in the presence of high concentrations of GdnHCl.

Supporting Information Available

RR spectra of Cyt c and its CL complex in the presence and absence of ethanol and the corresponding ethanol subtracted spectra; curve-fitting analysis of the high frequency region of the R 1:30 WT-CL complex spectrum; UV-vis and RR spectra of the R 1:30 CL complexes of the WT protein and the Cyt c K727379N, K7273N/H33Y, K7273N/H26Y, H2633N mutants; UV-vis and RR spectra of the Cyt c H2633N mutant; UV-vis and RR spectra of the ferrous WT protein and WT-CL R 1:30 complex; UV-Vis spectrum of the ferrous WT-CL R 1:30 CO adduct.

REFERENCES

(1) Hüttemann, M., Pecina, P., Rainbolt, M., Sanderson, T. H., Kagan, V. E., Samavati, L., Doan, J. W., and Lee, I. (2011) The multiple functions of Cytochrome c and their regulation in life and death decisions of the mammalian cell: from respiration to apoptosis. *Mitochondrion 11*, 369-381.

(2) Hannibal, L., Tomasina, F., Capdevila, D. A., Demicheli, V., Tórtora, V., Alvarez-Paggi, D., Jemmerson, R., Murgida, D. H., and Radi, R. (2016) Alternative conformations of Cytochrome *c* : structure, function, and detection. *Biochemistry 55*, 407–428.

(3) Sun, Y., Benabbas, A., Zeng, W., Kleingardner, J. G., Bren, K. L., and Champion, P. M. (2014) Investigations of heme distortion, low-frequency vibrational excitations, and electron transfer in Cytochrome c. *Proc. Natl. Acad. Sci. U. S. A 111*, 6570-6575.

(4) Kagan, V. E., Tyurin, V. A., Jiang, J., Tyurina, Y. Y., Ritov, V. B., Amoscato, A. A., Osipov, A. N., Belikova, N. A., Kapralov, A. A., Kini, V., Vlasova, I. I., Zhao, Q., Zou, M., Di, P., Svistunenko, D. A., Kurnikov, I. V, and Borisenko, G. G. (2005) Cytochrome c acts as a cardiolipin oxygenase required for release of proapoptotic factors. *Nat. Chem. Biol. 1*, 223–232.

(5) Rytömaa, M., and Kinnunen, P. K. J. (1994) Evidence for two distinct acidic phospholipid-binding sites in Cytochrome c. *J. Biol. Chem. 269*, 1770–1774.

(6) Rytomaa, M., and Kinnunen, P. K. J. (1995) Reversibility of the binding of Cytochrome c to liposomes. Implications for lipid-protein interactions. *J. Biol. Chem. 270*, 3197-3202.

(7) Tuominen, E. K. J., Wallace, C. J. A., and Kinnunen, P. K. J. (2002) Phospholipid-Cytochrome c interaction. Evidence for the extended lipid anchorage. *J. Biol. Chem. 277*, 8822–8826.

(8) Sinibaldi, F., Howes, B. D., Piro, M. C., Polticelli, F., Bombelli, C., Ferri, T., Coletta, M., Smulevich, G., and Santucci, R. (2010) Extended cardiolipin anchorage to Cytochrome c: a model for protein-mitochondrial membrane binding. *J. Biol. Inorg. Chem. 15*, 689–700.

(9) Kawai, C., Prado, F. M., Nunes, G. L. C., Di Mascio, P., Carmona-Ribeiro, A. M., and Nantes, I. L. (2005) pH-dependent interaction of Cytochrome c with mitochondrial mimetic membranes:

The role of an array of positively charged amino acids. *J. Biol. Chem. 280*, 34709–34717.

(10) Kagan, V. E., Bayir, H. A., Belikova, N. A., Kapralov, O., Tyurina, Y. Y., Tyurin, V. A., Jiang, J., Stoyanovsky, D. A., Wipf, P., Kochanek, P. M., Greenberger, J. S., Pitt, B., Shvedova, A. A., and Borisenko, G. (2009) Cytochrome c/cardiolipin relations in mitochondria: a kiss of death. *Free Radic. Biol. Med. 46*, 1439–1453.

(11) O'Brien, E. S., Nucci, N. V., Fuglestad, B., Tommos, C., and Wand, A. J. (2015) Defining the apoptotic trigger: the interaction of Cytochrome c and cardiolipin. *J. Biol. Chem. 290*, 30879–30887.

(12) Hanske, J., Toffey, J. R., Morenz, A. M., Bonilla, A. J., Schiavoni, K. H., and Pletneva, E. V. (2012) Conformational properties of cardiolipin-bound Cytochrome c. *Proc. Natl. Acad. Sci. 109*, 125–130.

(13) Milorey, B., Serpas, L., Pandiscia, L., and Schweitzer-Stenner, R. (2016) Exploring oxidation state dependent conformational changes of Cytochrome c on cardiolipin containing liposomes. *Biophys. J. 110*, 422a.

(14) Kapetanaki, S. M., Silkstone, G., Husu, I., Liebl, U., Wilson, M. T., and Vos, M. H. (2009) Interaction of carbon monoxide with the apoptosis-inducing Cytochrome c-cardiolipin complex. *Biochemistry 48*, 1613–1619.

(15) Bradley, J. M., Silkstone, G., Wilson, M. T., Cheesman, M. R., and Butt, J. N. (2011) Probing a complex of Cytochrome c and cardiolipin by magnetic circular dichroism spectroscopy: Implications for the initial events in apoptosis. *J. Am. Chem. Soc. 133*, 19676–19679.

(16) Sinibaldi, F., Droghetti, E., Polticelli, F., Piro, M. C., Di Pierro, D., Ferri, T., Smulevich, G., and Santucci, R. (2011) The effects of ATP and sodium chloride on the Cytochrome c-cardiolipin interaction: The contrasting behavior of the horse heart and yeast proteins. *J. Inorg. Biochem. 105*, 1365–1372.

(17) Capdevila, D. A., Oviedo Rouco, S., Tomasina, F., Tórtora, V., Demicheli, V., Radi, R., and Murgida, D. H. (2015) Active site structure and peroxidase activity of oxidatively-modified

Cytochrome c species in complexes with cardiolipin. *Biochemistry 54*, 7491-7504.

(18) Bergstrom, C. L., Beales, P. A., Lv, Y., Vanderlick, T. K., and Groves, J. T. (2013) Cytochrome c causes pore formation in cardiolipin-containing membranes. *Proc. Natl. Acad. Sci. U. S. A. 110*, 6269–74.

(19) Jemmerson, R., Liu, J., Hausauer, D., Lam, K. P., Mondino, A., and Nelson, R. D. (1999) A conformational change in Cytochrome c of apoptotic and necrotic cells is detected by monoclonal antibody binding and mimicked by association of the native antigen with synthetic phospholipid vesicles. *Biochemistry 38*, 3599–3609.

(20) Ranieri, A., Millo, D., Di Rocco, G., Battistuzzi, G., Bortolotti, C. A., Borsari, M., and Sola, M. (2015) Immobilized Cytochrome c bound to cardiolipin exhibits peculiar oxidation state-dependent axial heme ligation and catalytically reduces dioxygen. *J. Biol. Inorg. Chem. 20*, 531–540.

(21) Sinibaldi, F., Howes, B. D., Piro, M. C., Caroppi, P., Mei, G., Ascoli, F., Smulevich, G., and Santucci, R. (2006) Insights into the role of the histidines in the structure and stability of Cytochrome c. *J. Biol. Inorg. Chem. 11*, 52–62.

(22) Sinibaldi, F., Howes, B. D., Droghetti, E., Polticelli, F., Piro, M. C., Di Pierro, D., Fiorucci, L., Coletta, M., Smulevich, G., and Santucci, R. (2013) Role of lysines in cytochrome c-cardiolipin interaction. *Biochemistry 52*, 4578–88.

(23) Sinibaldi, F., Piro, M. C., Howes, B. D., Smulevich, G., Ascoli, F., and Santucci, R. (2003) Rupture of the hydrogen bond linking two Ω-loops induces the molten globule state at neutral pH in Cytochrome c. *Biochemistry 42*, 7604–7610.

(24) Ciaccio, C., Tognaccini, L., Battista, T., Cervelli, M., Howes, B. D., Santucci, R., Coletta, M., Mariottini, P., Smulevich, G., and Fiorucci, L. (2017) The Met80Ala and Tyr67His / Met80Ala mutants of human cytochrome c shed light on the reciprocal role of Met80 and Tyr67 in regulating ligand access into the heme pocket. *J. Inorg. Biochem. 169*, 86–96.

(25) Margoliash, E., and Frohwirt, N. (1959) Spectrum of horse-heart Cytochrome c. *Biochem. J.*

71, 570–572.

(26) Oellerich, S., Wackerbarth, H., and Hildebrandt, P. (2002) Spectroscopic characterisation of nonnative conformational states of Cytochrome c. *J.Phys.Chem.B 106*, 6566–6580.

(27) Belikova, N. A., Vladimirov, Y. A., Osipov, A. N., Kapralov, A. A., Tyurin, V. A., Potapovich, M. V., Basova, L. V., Peterson, J., Kurnikov, I. V., and Kagan, V. E. (2006) Peroxidase activity and structural transitions of Cytochrome c bound to cardiolipin-containing membranes. *Biochemistry 45*, 4998–5009.

(28) Hong, Y., Muenzner, J., Grimm, S. K., and Pletneva, E. V. (2012) Origin of the conformational heterogeneity of cardiolipin-bound Cytochrome c. *J. Am. Chem. Soc. 134*, 18713–18723.

(29) Trusova, V. M., Gorbenko, G. P., Molotkovsky, J. G., and Kinnunen, P. K. J. (2010) Cytochrome c-lipid interactions: new insights from resonance energy transfer. *Biophys. J. 99*, 1754–1763.

(30) Pandiscia, L. A., and Schweitzer-Stenner, R. (2015) Coexistence of native-like and non-native Cytochrome c on anionic liposomes with different cardiolipin content. *J. Phys. Chem. B 119*, 12846–12859.

(31) Brautigan, D. L., Feinberg, B. A., Hoffman, B. M., Margoliash, E., Peisach, J., and Blumberg, W E. (1977) Multiple Low Spin Forms of the Cytochrome c Ferrihemoehrome. *J. Biol. Chem. 252*, 574–582.

(32) Santoni, E., Scatragli, S., Sinibaldi, F., Fiorucci, L., Santucci, R., and Smulevich, G. (2004) A model for the misfolded bis-His intermediate of Cytochrome c: the 1-56 N-fragment. *J. Inorg. Biochem. 98*, 1067–1077.

(33) Gadsby, P. M., Peterson, J., Foote, N., Greenwood, C., and Thomson, A. J. (1987) Identification of the ligand-exchange process in the alkaline transition of horse heart Cytochrome c. *Biochem. J. 246*, 43–54.

(34) Othman, S., Le Lirzin, A., and Desbois, A. (1994) Resonance Raman investigation of

imidazole and imidazolate complexes of microperoxidase: characterization of the bis(histidine) axial ligation in c- type Cytochromes. *Biochemistry 33*, 15437–15448.

(35) Mitchell, M. L., Li, X.-Y., Kincaid, J. R., and Spiro, T. G. (1987) Axial ligand and out-of-plane vibrations for bis(imidazolyl)heme - Raman and infrared ^{54}Fe, ^{15}N, and ^{2}H isotope shifts and normal coordinate calculations. *J. Phys. Chem. 91*, 4690–4696.

(36) Jentzen, W., Ma, J., and Shelnutt, J. A. (1998) Conservation of the conformation of the porphyrin macrocycle in hemoproteins. *Biophys. J. 74*, 753–763.

(37) Shelnutt, J. A., Song, X., Ma, J., and Jia, S. (1998) Nonplanar porphyrins and their significance in proteins *Chem. Soc. Rev. 27*, 31–41.

(38) Döpner, S., Hildebrandt, P., Resell, F. I., and Mauk, A. G. (1998) Alkaline conformational transitions of ferricytochrome c studied by resonance Raman spectroscopy. *J. Am. Chem. Soc. 120*, 11246–11255.

(39) Hu, S., Morris, I., and Singh, J. (1993) Complete assignment of Cytochrome c resonance Raman spectra via enzymic reconstitution with isotopically labeled hemes. *J. Am. Chem. Soc. 115*, 12446–12458.

(40) Oellerich, S., Wackerbarth, H., and Hildebrandt, P. (2003) Conformational equilibria and dynamics of Cytochrome c induced by binding of sodium dodecyl sulfate monomers and micelles. *Eur. Biophys. J. 32*, 599–613.

(41) Kraus, D. W., and Wittenberg, J. B. (1990) Hemoglobins of the Lucina pectinata/bacteria symbiosis: I. Molecular properties, kinetics and equilibria of reactions with ligands. *J. Biol. Chem. 265*, 16043–16053.

(42) Blumberg, W. E., Peisach, J., Wittenberg, B. A., and Wittenberg, J. B. (1968) The electronic structure of protoheme proteins. I. An electron paramagnetic resonance and optical study of horseradish peroxidase and its derivatives. *J. Biol. Chem. 243*, 1854–1862.

(43) Howes, B. D., Feis, A., Indiani, C., Marzocchi, M. P., and Smulevich, G. (2000) Formation of two types of low-spin heme in horseradish peroxidase isoenzyme A2 at low temperature. *J. Biol.*

Inorg. Chem. 5, 227–235.

(44) Serpas, L., Milorey, B., Pandiscia, L. A., Addison, A. W., and Schweitzer-Stenner, R. (2016) Autoxidation of reduced horse heart Cytochrome *c* catalyzed by cardiolipin-containing membranes. *J. Phys. Chem. B*, DOI: 10.1021/acs.jpcb.6b05620.

(45) Tognaccini, L., Ciaccio, C., D'oria, V., Cervelli, M., Howes, B. D., Coletta, M., Mariottini, P., Smulevich, G., and Fiorucci, L. (2016) Structure–function relationships in human Cytochrome c: the role of tyrosine 67. *J. Inorg. Biochem. 155*, 56–66.

(46) Kitagawa, T. (1988) The heme protein structure and the iron histidine stretching mode, in *Biological applications of Raman spectroscopy: resonance Raman spectra of hemes and metalloproteins* (Spiro, T. G., Ed.) vol. 3, pp. 97-131, John Wiley and Sons Inc, New York.

(47) Stein, P., Mitchell, M., and Spiro, T. G. (1980) H-Bond and deprotonation effects on the resonance Raman iron-imidazol mode in deoxyhemoglobin models: implications for hemoglobin cooperativity. *J. Am. Chem. Soc. 102*, 7795–7797.

(48) Teraoka, J., and Kitagawa, T. (1980) Resonance raman study of the heme-linked ionization in reduced horseradish peroxidase. *Biochem. Biophys. Res. Commun. 93*, 694–700.

(49) Kitagawa, T., Nagai, K., and Tsubaki, M. (1979) Assignment of the Fe-Nε (His F8) stretching band in the resonance Raman spectra of deoxy myoglobin. *FEBS Lett. 104*, 376–378.

(50) Bushnell, G. W., Louie, G. V, and Brayer, G. D. (1990) High-resolution three-dimensional structure of horse heart Cytochrome c. *J. Mol. Biol. 214*, 585–595.

(51) Spiro, T. G., and Wasbotten, I. H. (2005) CO as a vibrational probe of heme protein active sites. *J. Inorg. Biochem. 99*, 34–44.

(52) Kerr, E. A., and Yu, N.-T. (1988) Vibrational modes of coordinated CO, CN^-, O_2 and NO, in *Biological applications of Raman spectroscopy: resonance Raman spectra of hemes and metalloproteins* (Spiro, T. G., Ed.) vol. 3, pp. 39-95, John Wiley and Sons Inc, New York.

(53) Phillips, G. N., Teodoro, M. L., Li, T., Smith, B., and Olson, J. S. (1999) Bound CO is a molecular probe of electrostatic potential in the distal pocket of myoglobin. *J. Phys. Chem. B 103*,

8817–8819.

(54) Kalanxhi, E., and Wallace, C. J. A. (2007) Cytochrome c impaled: investigation of the extended lipid anchorage of a soluble protein to mitochondrial membrane models. *Biochem. J. 407*, 179–187.

(55) Balakrishnan, G., Hu, Y., and Spiro, T. G. (2012) His26 protonation in Cytochrome c triggers microsecond β-sheet formation and heme exposure: implications for apoptosis. *J. Am. Chem. Soc. 134*, 19061–19069.

(56) Caroppi, P., Sinibaldi, F., Santoni, E., Howes, B. D., Fiorucci, L., Ferri, T., Ascoli, F., Smulevich, G., and Santucci, R. (2004) The 40s Ω-loop plays a critical role in the stability and the alkaline conformational transition of Cytochrome c. *J. Biol. Inorg. Chem. 9*, 997–1006.

(57) Muenzner, J., Toffey, J. R., Hong, Y., and Pletneva, E. V. (2013) Becoming a peroxidase: cardiolipin-induced unfolding of Cytochrome c. *J. Phys. Chem. B 117*, 12878–12886.

(58) Krishna, M. M. G., Maity, H., Rumbley, J. N., Lin, Y., and Englander, S. W. (2006) Order of steps in the Cytochrome c folding pathway: evidence for a sequential stabilization mechanism. *J. Mol. Biol. 359*, 1410–1419.

(59) Russell, B. S., Melenkivitz, R., and Bren, K. L. (2000) NMR investigation of ferriCytochrome c unfolding: detection of an equilibrium unfolding intermediate and residual structure in the denatured state. *Proc. Natl. Acad. Sci. U. S. A. 97*, 8312–8317.

(60) Russell, B. S., and Bren, K. L. (2002) Denaturant dependence of equilibrium unfolding intermediates and denatured state structure of horse ferriCytochrome c. *J. Biol. Inorg. Chem. 7*, 909–916.

(61) Yeh, S., Han, S., and Rousseau, D. (1998) Cytochrome c folding and unfolding: a biphasic mechanism. *Acc. Chem. Res. 31*, 727–736.

(62) Colón, W., Wakem, L. P., Sherman, F., and Roder, H. (1997) Identification of the predominant non-native histidine ligand in unfolded Cytochrome c. *Biochemistry 36*, 12535–12541.

(63) Fedurco, M., Augustynski, J., Indiani, C., Smulevich, G., Antalík, M., Bánó, M., Sedlák, E.,

Glascock, M. C., and Dawson, J. H. (2004) The heme iron coordination of unfolded ferric and ferrous Cytochrome c in neutral and acidic urea solutions. Spectroscopic and electrochemical studies. *Biochim. Biophys. Acta - Proteins Proteomics 1703*, 31–41.

(64) Banci, L., Bertini, I., Rosato, A., and Varani, G. (1999) Mitochondrial Cytochromes c: a comparative analysis. *J. Biol. Inorg. Chem. 4*, 824–837.

For Table of Contents Use Only

Unravelling the non-native low spin state of the cytochrome c – cardiolipin complex: evidence for the formation of a His ligated species only

Lisa Milazzo, Lorenzo Tognaccini, Barry D. Howes, Federica Sinibaldi, Maria C. Piro, Maria Fittipaldi, Maria C. Baratto, Rebecca Pogni, Roberto Santucci, and Giulietta Smulevich

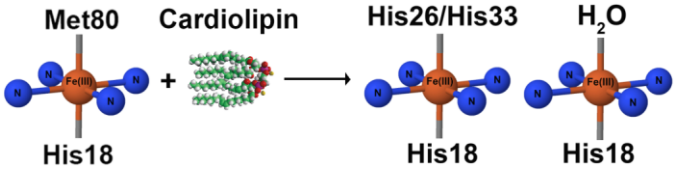

Supporting Information

Unravelling the non-native low spin state of the cytochrome c – cardiolipin complex: evidence for the formation of a His ligated species only

Lisa Milazzo,[†] Lorenzo Tognaccini,[†] Barry D. Howes,[†] Federica Sinibaldi,[‡] Maria C. Piro,[‡] Maria Fittipaldi,[§] Maria C. Baratto,[≠] Rebecca Pogni,[≠] Roberto Santucci,[⊥] and Giulietta Smulevich[*,†]

[†]Dipartimento di Chimica "Ugo Schiff", Università di Firenze, Via della Lastruccia 3-13, 50019 Sesto Fiorentino, Italy

[‡]Dipartimento di Scienze Cliniche e Medicina Traslazionale, Università di Roma 'Tor Vergata', Via Montpellier 1, 00133 Rome, Italy

[§]Dipartimento di Fisica ed Astronomia, Università di Firenze, Via Sansone 1, 50019 Sesto Fiorentino (FI), Italy

[≠]Dipartimento di Biotecnologie, Chimica e Farmacia, Università di Siena, via Aldo Moro 2, 53100 Siena, Italy

[⊥]Dipartimento di Scienze Cliniche e Medicina Traslazionale, Università di Roma 'Tor Vergata', Via Montpellier 1, 00133 Rome, Italy

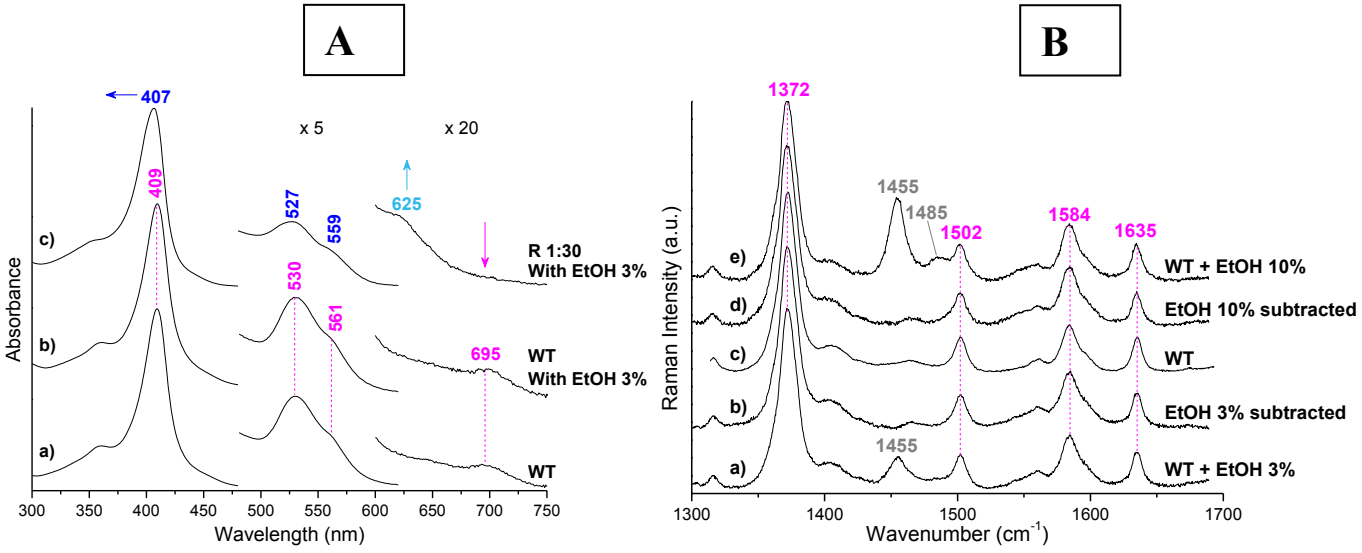

Figure S1.

A) UV-Vis spectra of the ferric WT protein without (a) and with ethanol (b) and of the ferric WT-CL R 1:30 complex (c). The ethanol concentration in spectra (b) and (c) is 3% v/v.

The band wavelengths of the His-Fe-Met native species, the His-Fe-His species and the 6cHS species are shown in magenta, blue and light blue, respectively. The 470–620 nm and the 600-750 nm regions of the spectra are expanded 5-fold and 20-fold, respectively. The spectra have been shifted along the ordinate axis to allow better visualization.

B) RR spectra at 298 K in the high frequency region of the ferric WT protein without (c) and with 3% (a) and 10% (e) ethanol v/v. The same spectra after ethanol 3% and 10% v/v subtraction (b and d, respectively) are also shown. The band frequencies of the His-Fe-Met native species and ethanol are shown in magenta and grey, respectively. The spectra have been shifted along the ordinate axis to allow better visualization and the intensity of the spectra is normalized to that of the ν_4 band. Experimental conditions: excitation wavelength 406.7 nm, laser power at the sample 5 mW, average of 5 spectra with 50 min integration time (a), average of 5 spectra with 25 min integration time (c), and average of 4 spectra with 40 min integration time (e).

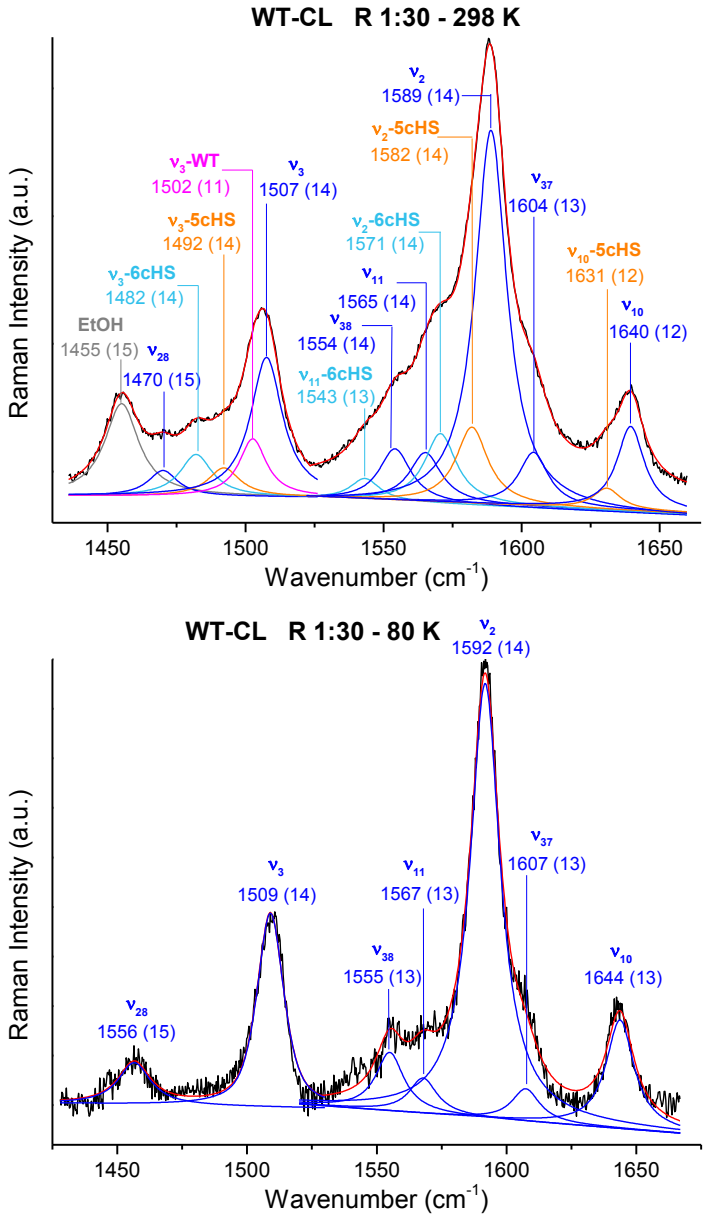

Figure S2. Curve-fitting analysis of the 1430-1670 cm^{-1} high frequency region of the R 1:30 WT-CL complex spectrum at 298 K (top) and at 80 K (bottom). The frequencies of the bands due to the 6cLS His-Fe-Met native species, the 6cLS bis-His species, the 6cHS and the 5cHS species are shown in magenta, blue, light blue and orange, respectively. The spectrum at 298 K was obtained using a spherical lens while that at 80 K was obtained using a cylindrical lens. Experimental conditions: 20 mM Hepes pH 7.0,

excitation wavelength 406.7 nm, laser power at the sample 5 mW; average of 21 spectra with 105 min integration time (298 K) and average of 20 spectra with 100 min integration time (80 K).

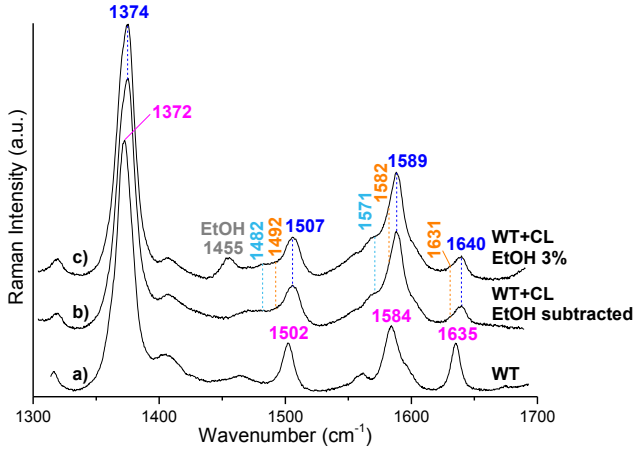

Figure S3. RR spectra at 298 K in the high frequency region of the ferric WT protein (a) and the WT-CL R 1:30 complex (c). The difference spectrum of the WT-CL R 1:30 complex without ethanol is also shown (b). The band frequencies due to the His-Fe-Met native species, the His-Fe-His species, the 6cHS, the 5cHS species, and ethanol are shown in magenta, blue, light blue, orange, and grey, respectively. The spectra have been shifted along the ordinate axis to allow better visualization and the intensity of the spectra is normalized to that of the ν_4 band. Experimental conditions: excitation wavelength 406.7 nm, laser power at the sample 5 mW, average of 5 spectra with 25 min integration time (a) and average of 21 spectra with 105 min integration time (c). The ethanol concentration in spectrum c is of 3% v/v. The ethanol concentration in spectrum (c) is of 3% v/v.

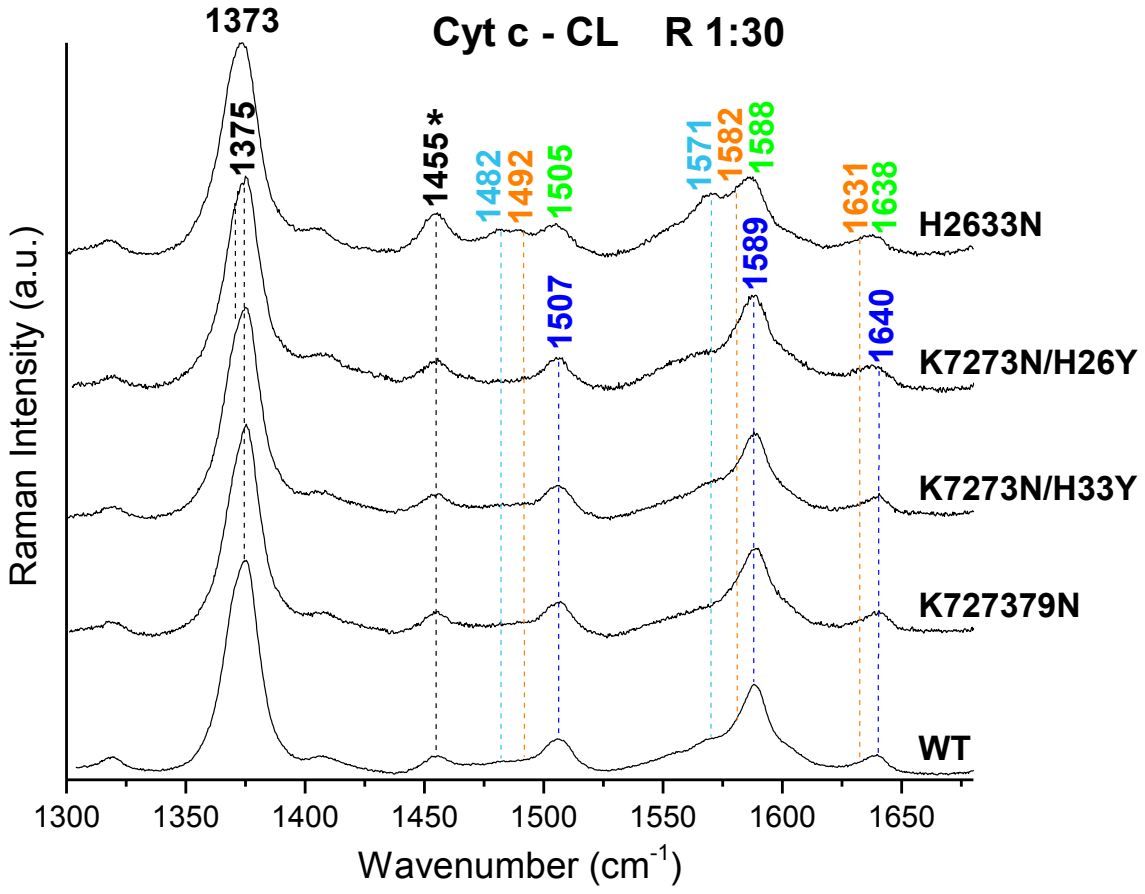

Figure S4. RR spectra at 298 K in the high frequency region of the R 1:30 CL complexes of the WT protein and of the Cyt c K727379N, K7273N/H33Y, K7273N/H26Y, and H2633N mutants. The frequencies of the bands due to the bis-His species, the OH^--Fe-His species, the 6cHS and the 5cHS species are shown in blue, green, light blue and orange, respectively. The spectra have been shifted along the ordinate axis to allow better visualization and the intensity of the spectra is normalized to that of the ν_4 band. Experimental conditions: 20 mM Hepes pH 7.0, excitation wavelength 406.7 nm, laser power at the sample 5 mW; average of 21 spectra with 105 min integration time (WT), average of 12 spectra with 60 min integration time (K727379N), average of 18 spectra with 90 min integration time (K7273N/H33Y), average of 14 spectra with 70 min integration time (K7273N/H26Y), average of 7 spectra with 35 min integration time (H2633N).

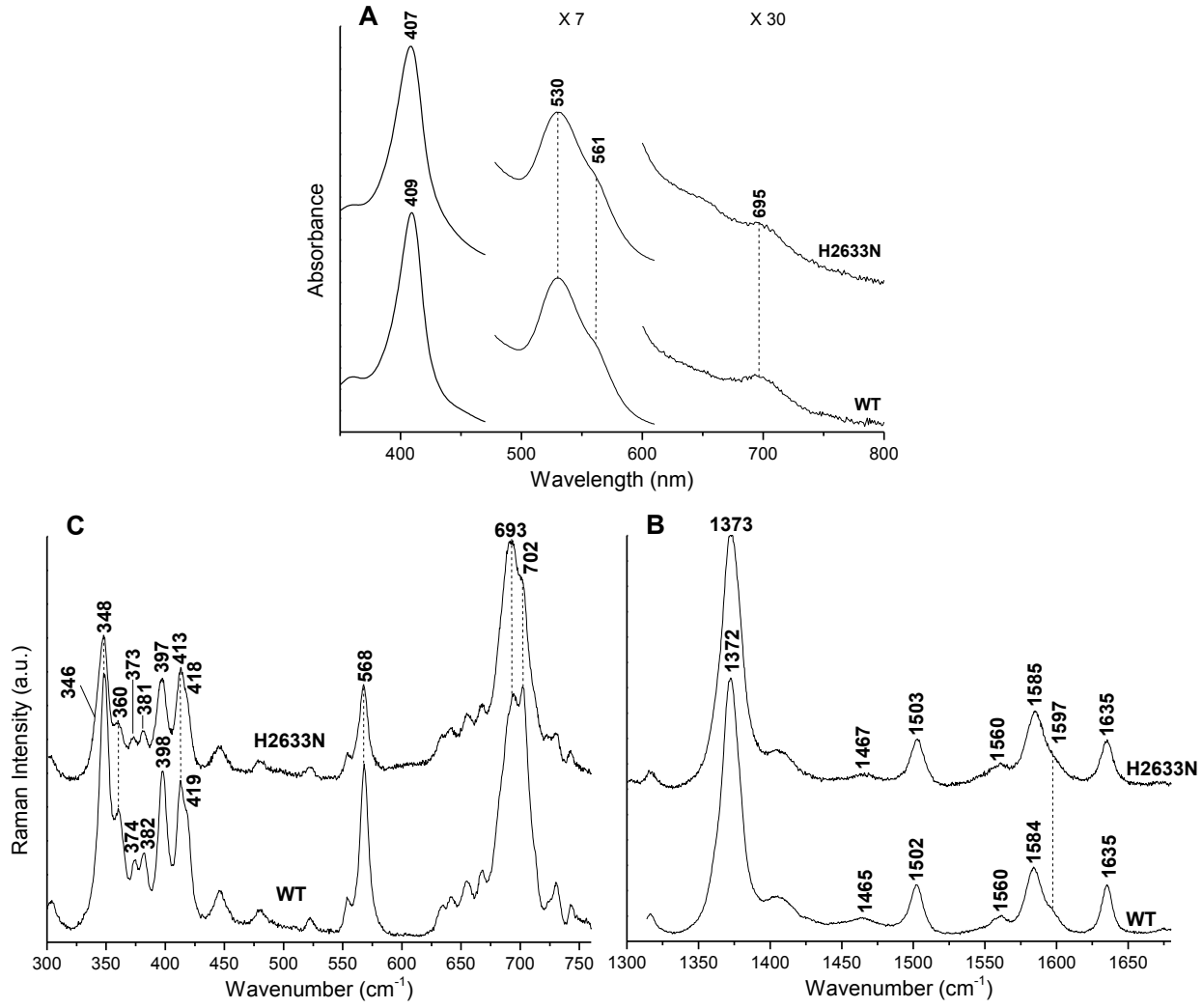

Figure S5. UV-vis (panel A) and RR spectra at 298 K in the high (panel B) and low (panel C) frequency regions of the Cyt c H2633N mutant. The spectra of the WT protein are also shown for comparison. The spectra have been shifted along the ordinate axis to allow better visualization. In panel A the 470–620 nm and the 600–800 nm regions of the spectra are expanded 7-fold and 30-fold, respectively. In panels B and C the intensity of the spectra is normalized to that of the ν_4 band. RR experimental conditions: 20 mM Hepes pH 7.0, 298 K, excitation wavelength 406.7 nm, laser power at the sample 5 mW; **WT**: average of 5 spectra with 25 min integration time (B) and average of 4 spectra with 20 min integration time (C); **H2633N**: average of 19 spectra with 95 min integration time (B) and average of 18 spectra with 90 min integration time (C).

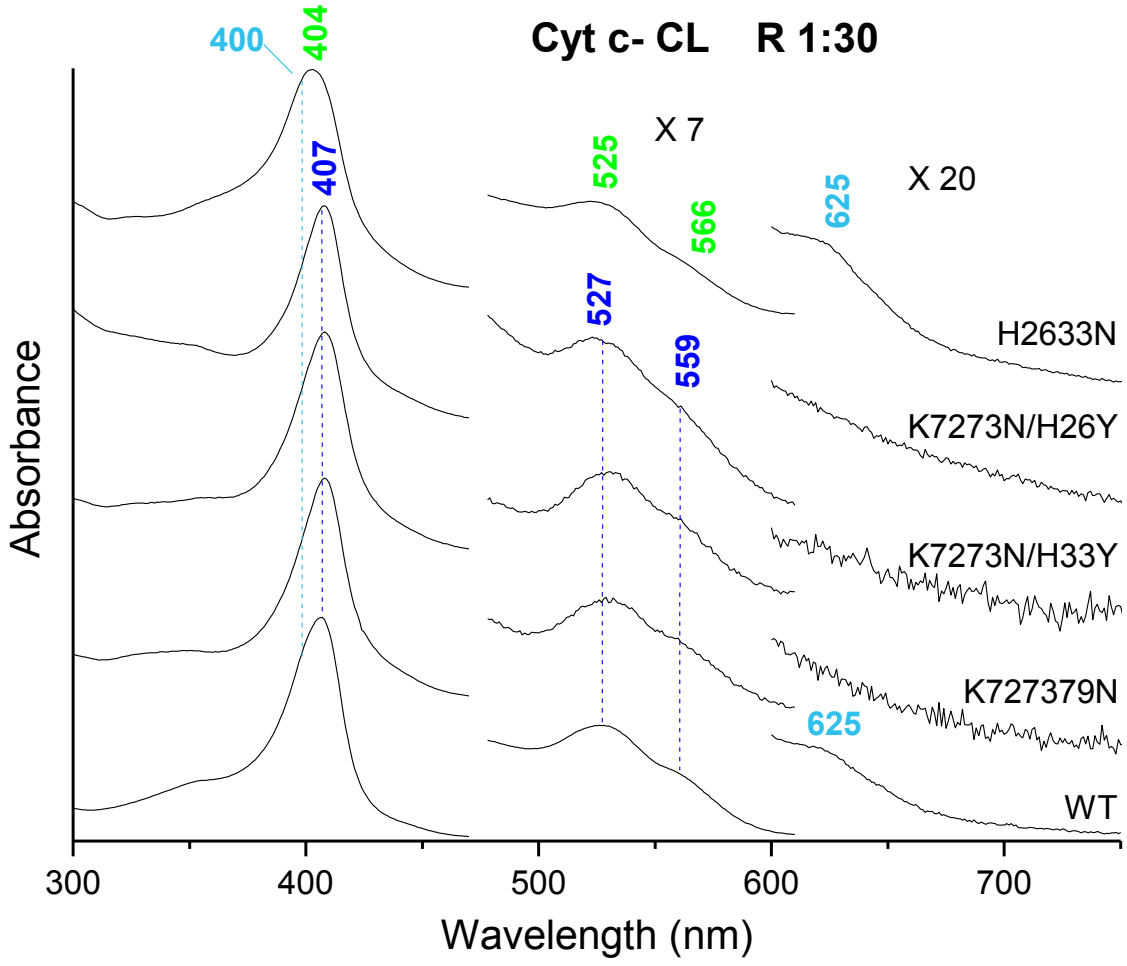

Figure S6. UV-vis spectra of the R 1:30 CL complexes of the WT protein and the Cyt c K727379N, K7273N/H33Y, K7273N/H26Y, H2633N mutants. The wavelengths of the bands assigned to the bis-His species, the OH^--Fe-His species and the 6cHS species are shown in blue, green and light blue, respectively. The 470–620 nm and the 600–750 nm regions of the spectra are expanded 7-fold and 20-fold, respectively. The spectra have been shifted along the ordinate axis to allow better visualization.

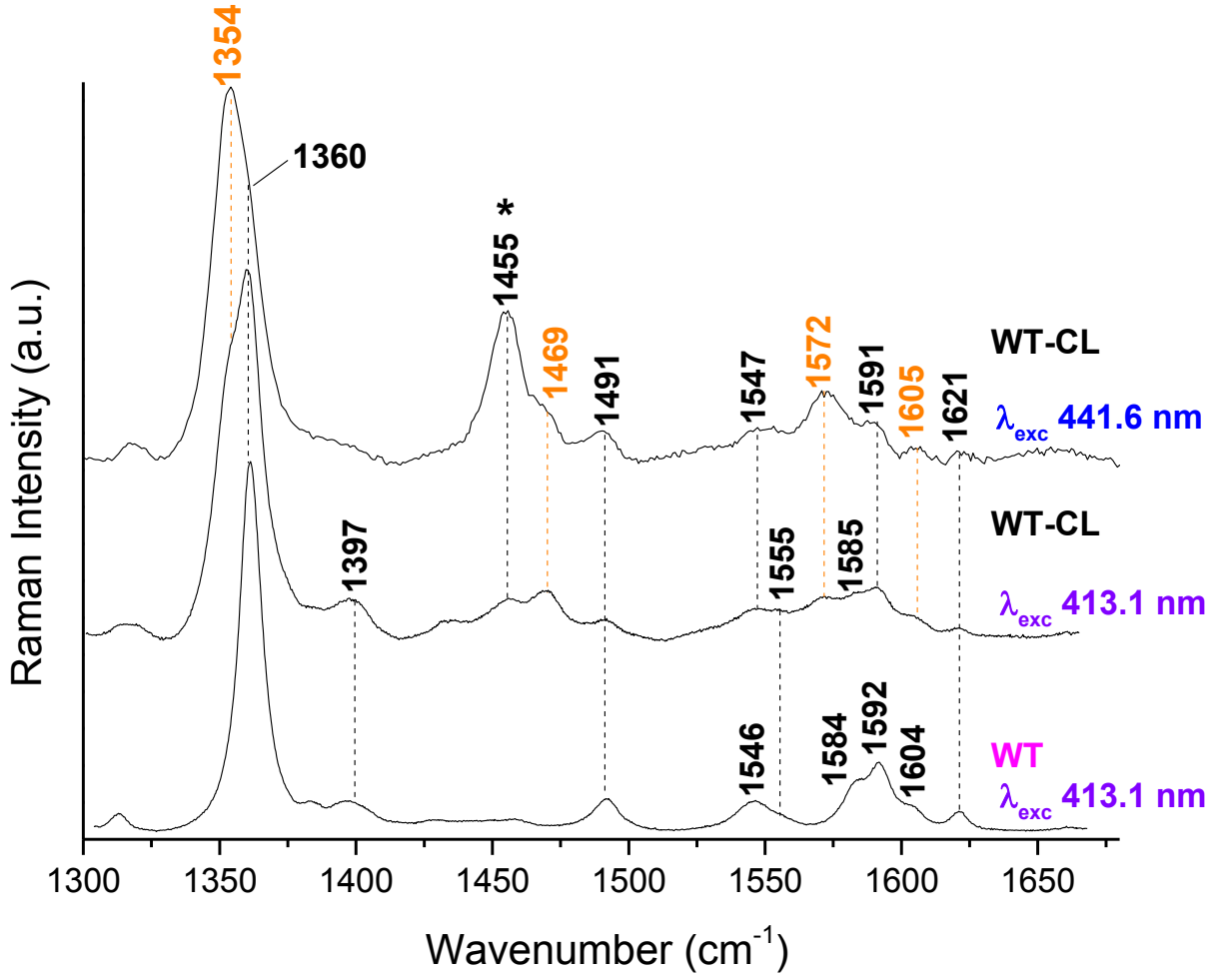

Figure S7. RR spectra at 298 K in the high frequency region of the ferrous WT protein (λ_{exc} 413.1 nm) and the WT-CL R 1:30 complex (λ_{exc} 413.1 nm and λ_{exc} 441.6 nm). The frequencies of the bands assigned to the 5cHS species are shown in orange. The spectra have been shifted along the ordinate axis to allow better visualization and the intensity of the spectra is normalized to that of the ν_4 band. Experimental conditions: **WT**: excitation wavelength 413.1 nm, laser power at the sample 5 mW, average of 4 spectra with 20 min integration time; **WT-CL**: laser power at the sample 6 mW, average of 15 spectra with 75 min integration time (λ_{exc} 413.1 nm) and laser power at the sample 26 mW, average of 3 spectra with 15 min integration time with a 1800 grooves/mm grating (λ_{exc} 441.6 nm).

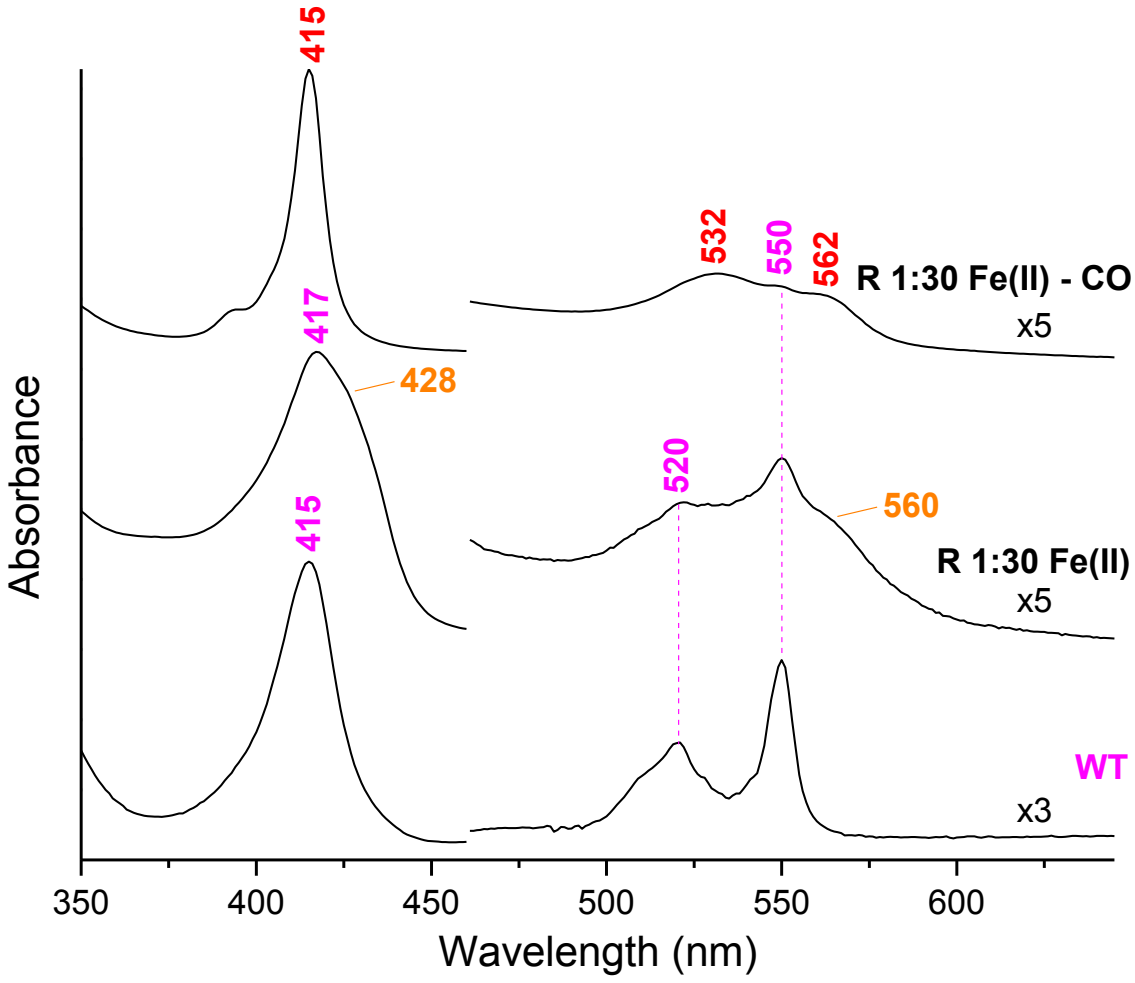

Figure S8. UV-vis spectra of the ferrous WT protein, the WT-CL R 1:30 complex and the WT-CL R 1:30 CO adduct. The wavelengths of the bands assigned to the His-Fe-Met native species, to the 5cHS species and to the CO complex are shown in magenta, orange and red, respectively. The 470–650 nm region of the spectra is expanded 3- or 5-fold. The spectra have been shifted along the ordinate axis to allow better visualization.